compounds. Therefore, ABCG2 may have a distinct role in efflux transport at the BBB.

Several ABC transporters and organic anion transporters are expressed at the abluminal and/or luminal membrane of the BBB as well as ABCG2 (Gao *et al.* 1999; Virgintino *et al.* 2002; Mori *et al.* 2003). Clarifying the transport properties and the contribution of each transporter at the BBB is an important issue for understanding the physiological roles of these molecules. However, the substrate and inhibitor specificities of these transporters sometimes overlap. For example, dehydroepiandrosterone sulfate (DHEAS) is transported from brain to the circulating blood across the BBB via organic anion transporting polypeptide 2 (Asaba *et al.* 2000), while other transporters at the BBB, such as ABCG2 and ABCC4 (Zhang *et al.* 2000; Cooray *et al.* 2002; Hori *et al.* 2004), also accept DHEAS as a substrate (Suzuki *et al.* 2003; Zelcer *et al.* 2003).

Three effective inhibitors of ABCG2 have been described thus far. GF120918 was developed as a P-gp (ABCB1) inhibitor (Hyafil *et al.* 1993), but a later study found that it also inhibits ABCG2 (de Bruin *et al.* 1999). Such a dual-specificity inhibitor is unsuitable for clarifying the distinct transport activity of each transporter. Fumitoremorgin C and Ko143 are potent and selective inhibitors for ABCG2, being much less active towards P-gp and ABCCs (Rabindran *et al.* 2000; Allen *et al.* 2002). Nevertheless, the specificity of these inhibitors is concentration-dependent, and an influence of these two inhibitors on unidentified transporters at the BBB cannot be ruled out.

RNA interference is a conserved biological response to double-stranded RNA, which results in sequence-specific gene silencing (Hannon 2002). In mammalian cell cultures, double-stranded RNA-mediated interference with gene expression has also been accomplished by transfection of synthetic RNA oligonucleotides composed of 21 or 22 base pairs (short interfering RNA, siRNA; Elbashir *et al.* 2002). Sequence-specific silencing of transporter genes using siRNA should make it possible to evaluate properly the transport properties of a targeted transporter at the BBB.

Conditionally immortalized BCEC lines are useful *in vitro* BBB models which retain the *in vivo* transport properties towards various compounds (Hosoya *et al.* 2000a, 2000b; Terasaki *et al.* 2003). Endothelial cells are generally resistant to the introduction of exogenous DNA, and molecular analysis of endothelial cells has been hampered by the difficulty of transiently transfecting genes with high efficiency. Therefore, siRNA-induced specific knockdown of target transporter genes in BCECs should allow us to improve our understanding of the physiological and pharmacological functions of the efflux transport systems at the BBB.

The purpose of this study was therefore to specifically silence rABCG2 gene by the introduction of siRNA into BCECs, in order to clarify the role of ABCG2 at the BBB.

Materials and methods

Reagents

Endothelial cell growth factor (ECGF) was purchased from Boehringer Mannheim (Mannheim, Germany). Benzylpenicillin potassium and streptomycin sulfate were purchased from Wako Pure Chemical Industries (Osaka, Japan). Non-specific Control Duplex XI (NC siRNA; Dharmacon, Lafayette, CO, USA) is claimed by the manufacturer to show no RNAi effect, and its target sequence is 5′-NNATAGATAAGCAAGCCTTAC-3′. No rat gene sequences with homology to NC siRNA were found by Blast search. β-Actin siRNA was purchased from Qiagen (Tokyo, Japan); its target sequence is 5′-AATGAAGATCAAGATCATTGC-3′. The sequence of β-actin siRNA is identical at 20 bp out of 21 bp with the corresponding sequence of rat β-actin (the underlined base in the sequence of β-actin siRNA is changed to 'C' in that of rat β-actin). All other chemicals were commercial products of analytical grade.

siRNA preparation

Four different siRNA duplexes were designed based on the coding sequence of rABCG2 cDNA (GenBank accession number AB105817). All 21-nucleotides (nt) siRNAs contained 3′-dTdT extensions and their GC contents were less than 70%. The sequences, positions and GC contents of siRNA targeting rat ABCG2 are shown in Table 1. All of the siRNA duplexes were

Table 1 Sequences of rABCG2 short interfering RNAs (siRNAs)

Number of rABCG2 siRNA	Sequences (upper, sense; lower, antisense)	Positions*/GC (%)
01	5′-CAGAGAAACAAGAACGGCCdTdT dTdTGUCUCUUUGUUCUUGCCGG-5′	95–113/52.6%
02	5′-UGUGCUAAGUUUUCAUCACdTdT dTdTACACGAUUCAAAAGUAGUG-5′	160–178/36.8%
03	5′-CCCUGACAGUGAGAGAAAAdTdT dTdTGGGACUGUCACUCUCUUUU-5′	450–468/47.4%
04	5′-GCAAACAAGACAGAAGAGCdTdT dTdTCGUUUGUUCUGUCUUCUCG-5′	998–1016/47.4%

*GenBank accession number AB105817.

chemically synthesized and HPLC-purified by Proligo (La Jolla, CA, USA).

Cell culture

HEK293 cells (American Type Culture Collection, Rockville, MD, USA) were grown in Dulbecco's modified Eagle's medium (DMEM, Nissui Pharmaceutical, Tokyo, Japan) supplemented with 20 mM sodium bicarbonate, 100 U/mL benzylpenicillin potassium, 100 μg/mL streptomycin sulfate and 10% fetal bovine serum (Moregate, Bulimba, Australia; culture-medium A) at 37°C in a humidified atmosphere of 95% air and 5% CO_2. TR-BBB13 cells are a conditionally immortalized BCEC cell line (Hosoya *et al.* 2000a) that has been used as an *in vitro* BBB model (Terasaki *et al.* 2003). TR-BBB13 cells were grown in culture-medium A with 15 ng/mL ECGF. The cells were maintained at 33°C, which is a permissive temperature at which temperature-sensitive SV40 large T-antigen is activated, in a humidified atomosphere of 95% air and 5% CO_2.

Transfection of siRNA into HEK293 cells or TR-BBB13 cells

HEK293 cells were plated in six-well plates at 4×10^5 cells/well, grown for 24 h then transfected with 3 μg of rABCG2 siRNA-01, rABCG2 siRNA-02, rABCG2 siRNA-03, rABCG2 siRNA-04 or NC siRNA using Lipofectamine 2000 and OPTI-MEM I reduced serum medium (Invitrogen, Carlsbad, CA, USA). In some experiments, 1 μg of myc-tagged rABCG2 cDNA (pCMV-Tag3A/rABCG2 (Hori *et al.* 2004)) or a control plasmid (pCMV-Tag3A, Stratagene, La Jolla, CA, USA) was co-transfected into HEK293 cells simultaneously with siRNA. The mRNA expression and the transport activity were examined at 48 h after the transfection. The protein expression was examined at 24, 48 and 72 h after the transfection.

For quantitative real-time PCR analysis, TR-BBB13 cells were plated in six-well plates at 4×10^5 cells/well, grown for 24 h at 33°C then transfected with 4 μg of rABCG2 siRNA-03, β-actin siRNA or NC siRNA using Lipofectamine 2000 and OPTI-MEM I reduced serum medium (Invitrogen). At 24 h after siRNA transfection, TR-BBB13 cells were treated with or without 100 nM 17β-estradiol. Culture was continued for a further 24 h at 33°C. For western blot analysis, TR-BBB13 cells were plated in six-well plates at 4×10^5 cells/well, grown for 24 h at 33°C then transfected with 4 μg of rABCG2 siRNA-03 or NC siRNA using Lipofectamine 2000 and OPTI-MEM I reduced serum medium (Invitrogen). The protein expression was examined at 36 h after the transfection.

Quantitative real-time PCR analysis

Total RNA was extracted from HEK293 cells or TR-BBB13 cells with an RNeasy kit (Qiagen) according to the manufacturer's protocol. RNA integrity was checked by electrophoresis on an agarose gel. Single-stranded cDNA was prepared from 1 μg of total RNA by RT (ReverTraAce, Toyobo, Osaka, Japan) using oligo dT primer. Quantitative real-time PCR analysis was performed using an ABI PRISM 7700 sequence detector system (PE Applied Biosystems, Foster City, CA, USA) with 2 × SYBR Green PCR Master Mix (PE Applied Biosystems) according to the manufacturer's protocol. To quantify the amount of specific mRNA in the samples, standards for each run were prepared using pGEM-T Easy Vector containing ABCG2, ABCB1, ABCC1, ABCG1, β-actin or GAPDH (dilution ranging from 0.1 fg/μL to 1 ng/μL). The standard curves of each gene were obtained by linear regression between the logarithm of the standards of each gene and the corresponding threshold cycle (Ct) values. The Ct value indicates the cycle number at which the reaction begins to be exponential. All the plots showed high linearity, and the Ct values of all samples were within the range of the standard plots. The ABCG2, ABCB1, ABCC1 or ABCG1 mRNA levels were normalized relative to the β-actin mRNA level. The β-actin mRNA level was normalized relative to the GAPDH mRNA level. In Fig. 1, each rABCG2 mRNA level is indicated as a percentage of the mean of those in HEK293 cells co-transfected with NC siRNA and rABCG2 cDNA ($n = 3$; open column, NC+). In Fig. 4, each mRNA level is indicated as a percentage of the mean of mRNA levels in TR-BBB13 cells treated with non-siRNA (–) and 17β-estradiol (E2; $n = 3$; the leftmost column). The control lacking the RT enzyme was assayed in parallel to monitor any possible genomic contamination. The PCR was run for 40 cycles of 95°C for 30 s, 60°C for 1 min, and 72°C for 1 min after pre-incubation at 95°C for 10 min, using specific primers. The sequences of primers were as follows: sense primer 5′-CAATGGGATCATGAAACCTG-3′, antisense primer 5′-GAGGCTGATGAATGGAGAA-3′ for ABCG2; sense primer 5′-ACAGAAACAGAGGATCGC-3′ and antisense primer 5′-CGTCTTGATCATGTGGCC-3′ for ABCB1/mdr1a; sense primer 5′-CTGGCTTGGTGTGAACTGAT-3′ and antisense primer 5′-AGGCTCTGGCTTGGCTCTAT-3′ for ABCC1; sense primer 5′-TGCCCGCCGGGTTGAAACTGTTC-3′ and antisense primer 5′-ACTGTCTGCATTGCGTTGCATTGC-3′ for ABCG1; sense primer 5′-TTTGAGACCTTCAACACCCC-3′ and

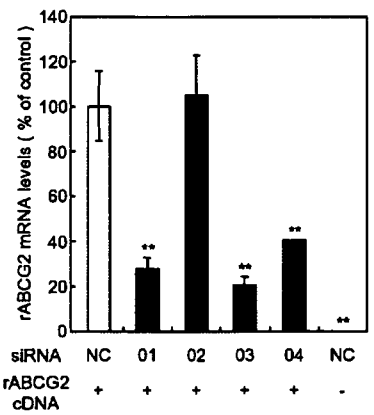

Fig. 1 Effects of rABCG2 siRNAs on the exogenous rABCG2 mRNA level in HEK293 cells co-transfected with myc-tagged rABCG2 cDNA. HEK293 cells were transfected with siRNAs (rABCG2 siRNA-01, rABCG2 siRNA-02, rABCG2 siRNA-03 and rABCG2 siRNA-04 (01, 02, 03 and 04) or non-specific control (NC) siRNA) with (+) or without (–) co-transfection of myc-tagged rABCG2 cDNA. At 48 h after transfection, the cells were collected for quantitative real-time PCR analysis. The sequences of rABCG2 siRNAs are shown in Table 1. Each column represents the mean ± SEM ($n = 3$). The rABCG2 mRNA level was normalized relative to the β-actin mRNA level. Each rABCG2 mRNA level is shown as percentage of the mean of the rABCG2 mRNA level in the NC siRNA-treated HEK293 cells cotransfected with myc-tagged rABCG2 cDNA (NC+). $^{**}p < 0.01$, significantly different from the NC+.

antisense primer 5′-ATAGCTCTTCTCCAGGGAGG-3′ for β-actin; sense primer 5′-TGATGACATCAAGAAGGTGGTGAAG-3′ and antisense primer 5′-TCCTTGGAGGCCATGTAGGCCAT-3′ for GAPDH.

Western blot analysis

HEK293 cells were lysed with lysis buffer containing 10 mM Tris–HCl (pH 7.4), 1 mM EDTA, 150 mM NaCl, 4% CHAPS, 1 mM phenylmethylsulfonyl fluoride, and a protease-inhibitor cocktail (Sigma Chemical Co., St Louis, MO, USA). The lysate was centrifuged at 15 000 *g* for 30 min and the supernatants were collected. TR-BBB13 cells were homogenized by mean of the nitrogen cavitation technique (800 psi, 15 min, 4°C) in buffer containing 10 mM HEPES-NaOH (pH 7.4), 250 mM sucrose, 1 mM EDTA, 1 mM phenylmethylsulphonyl fluoride (PMSF). The homogenized samples were centrifuged at 10 000 *g* for 10 min and the supernatants were collected. These supernatants were centrifuged at 100 000 *g* for 1 h, and a crude membrane fraction was obtained from the pellets. The pellets were suspended in lysis buffer. The protein concentration of samples was measured by the Bradford method using Bio-Rad Protein Assay reagent (Bio-Rad, Hercules, CA, USA). Protein samples (HEK293 cells, 12 μg; TR-BBB13 cells, 40 μg (for rABCG2) or 20 μg (for Na^+,K^+-ATPase and ABCB1) per lane) were resolved by 7.5% sodium dodecyl sulfate polyacrylamide gel electrophoresis (SDS–PAGE; Bio-Rad) and subsequently electrotransferred to nitrocellulose membranes. Membranes were treated with blocking buffer (4% skimmed milk in 25 mM Tris–HCl (pH 8.0), 125 mM NaCl, 0.1% Tween-20 for 2 h at 20°C and incubated with anti-c-myc antibody (0.1 μg/mL; Bethyl Laboratories Inc., Montgomery, TX, USA), anti-β-actin antibody (1 : 2000; Sigma), anti-Na^+,K^+-ATPase antibody (0.1 μg/mL; Upstate Biotechnology, Lake Placid, NY, USA), anti-ABCB1 antibody (C219) (1 : 100; Signet, Dedham, MA, USA), or anti-ABCG2 antibody (G2-Ab1) (1.0 μg/mL) (Hori *et al.* 2004) as the primary antibody at 4°C for 16 h after blocking. The membranes were washed three times with blocking buffer and incubated with horseradish peroxidase-conjugated second antibody. The bands were visualized with an enhanced chemiluminescence kit (SuperSignal; Pierce, Rockford, IL, USA). The relative densities of the bands were measured using NIH image software (National Institutes of Health, Bethesda, MD, USA).

Transport assay

For transport studies, HEK293 cells were incubated for 1 h at 37°C in a medium containing 20 μM mitoxantrone. The cells were then washed in ice-cold phosphate-buffered saline and placed on ice until measurement. Relative cellular accumulation of mitoxantrone was determined by flow cytometry with a 635 nm red diode laser and 661 nm bandpass filter (FACs Calibur, BD Biosciences, Lexington, KY, USA). A total of 20 000 events were collected. Debris was eliminated by gating on forward versus side scatter. The mean channel number for each histogram was used as a measure of drug fluorescence for calculation.

Data analysis

Unless otherwise indicated, all data represent the mean ± SEM. An unpaired, two-tailed Student's *t*-test was used to determine the significance of differences between two group means. One-way ANOVA followed by the modified Fisher's least-squares difference method was used to assess the statistical significance of differences among means of more than two groups.

Results

Silencing of exogenous rABCG2 gene in HEK293 cells

To determine the effects of four different siRNAs (rABCG2 siRNA-01, rABCG2 siRNA-02, rABCG2 siRNA-03 and rABCG2 siRNA-04; Table 1) on rABCG2 gene expression, quantitative real-time PCR analysis was performed using HEK293 cells co-transfected with myc-tagged rABCG2 cDNA. After treatment with rABCG2 siRNA-01, rABCG2 siRNA-03 or rABCG2 siRNA-04 for 48 h, the rABCG2 mRNA levels were suppressed in rABCG2-transfected HEK293 cells by 71.8%, 78.8% or 54.7%, respectively (01+, 03+ and 04+, Fig. 1), compared with those in cells treated with non-specific control (NC) siRNA (NC+, Fig. 1). In contrast, treatment with rABCG2 siRNA-02 had no significant effect on the rABCG2 mRNA level (02+, Fig. 1).

Effects of siRNAs on rABCG2 protein level in HEK293 cells

To clarify whether rABCG2 protein was reduced concomitantly with the suppression of rABCG2 mRNA, the level of exogenous rABCG2 protein was examined by western blot analysis. The protein was detected using anti-c-myc antibody, as rABCG2 protein was fused with the myc epitope. Myc tagged-rABCG2 proteins were detected at 80 kDa in HEK293 cells co-transfected with NC siRNA and myc-tagged rABCG2 cDNA (NC+, Fig. 2a), while no band was detected in HEK293 cells co-transfected with NC siRNA and the vector alone (i.e. without the myc-tagged rABCG2 cDNA insert) (NC–, Fig. 2a). rABCG2 siRNA-01, rABCG2 siRNA-03 and rABCG2 siRNA-04 each reduced the level of rABCG2 protein in HEK293 cells co-transfected with myc-tagged rABCG2 cDNA (01+, 03+ and 04+, Fig. 2a). rABCG2 siRNA-03 was the most effective (03+, Fig. 2a), and it reduced the relative density of the bands by 99.7 ± 0.1% (mean ± SEM; $n = 3$) compared with NC siRNA. In contrast, the rABCG2 protein level was not affected by rABCG2 siRNA-02 (02+, Fig. 2a). The level of β-actin protein was unchanged by any of the rABCG2 siRNAs (Fig. 2a). As shown in Figs 2(b and c), western blot analysis at 24 h and 72 h after transfection clearly demonstrated that co-transfection of rABCG2 siRNA-03, but not NC siRNA, significantly reduced the level of rABCG2 protein.

Effects of rABCG2 siRNAs on mitoxantrone efflux transport in rABCG2 cDNA-transfected HEK293 cells

Mean fluorescence intensity of mitoxantrone was significantly reduced in HEK293 cells following co-transfection with NC siRNA and myc-tagged rABCG2 cDNA (NC+, Fig. 3a) compared with NC siRNA alone (NC–, Fig. 3a). The proportion of transiently rABCG2 cDNA-transfected cells was 25.7 ± 0.4% (mean ± SEM; $n = 3$; gated area, Fig. 3b). rABCG2 siRNA-01, rABCG2 siRNA-03 and rABCG2 siRNA-04 significantly increased the mean fluorescence intensity of mitoxantrone (01+, 03+ and 04+, Fig. 3a), and indeed, rABCG2 siRNA-03 completely reversed the reduction of the mitoxantrone level. Representative histogram and dot plots showed that the population of rABCG2-transfected cells almost completely

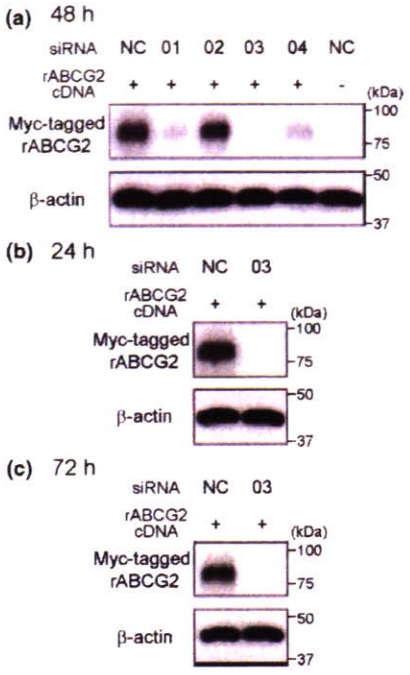

Fig. 2 Effects of rABCG2 siRNAs on exogenous rABCG2 protein in HEK293 cells co-transfected with myc-tagged rABCG2 cDNA. HEK293 cells were transfected with siRNAs (rABCG2 siRNA-01, rABCG2 siRNA-02, rABCG2 siRNA-03 and rABCG2 siRNA-04 (01, 02, 03 and 04) or non-specific control (NC) siRNA) with (+) or without (–) co-transfection of myc-tagged rABCG2 cDNA. The sequence of rABCG2 siRNAs are shown in Table 1. At 48 h (a), 24 h (b) or 72 h (c) after transfection, the cells were collected for western blot analysis using anti-c-myc and anti-β-actin antibodies. Typical results from repeated experiments are shown.

overlapped with that of non-transfected cells (03+, Fig. 3b). In contrast, rABCG2 siRNA-02 had no significant effect on the mean fluorescence intensity of mitoxantrone in HEK293 cells (02+, Fig. 3a).

Selective inhibition of endogenous rABCG2 gene in a conditionally immortalized BCEC line (TR-BBB13) by siRNA

rABCG2 siRNA-03, which is the most potent siRNA for attenuating rABCG2 function, was used to suppress endogenous rABCG2 expression in TR-BBB13 cells. At 24 h after siRNA transfection, TR-BBB13 cells were treated with 17β-estradiol, which has been reported to induce ABCG2 mRNA expression in cancer cells (Ee *et al.* 2004), or not treated. In the absence of 17β-estradiol, the rABCG2 mRNA level was reduced by 42.2% by transfection of rABCG2 siRNA-03 into TR-BBB13 cells (G2-03), whereas transfection of NC siRNA had no effect (NC)[E_2(–), Fig. 4a]. The rABCG2 mRNA level was significantly induced in non-siRNA-transfected TR-BBB13 cells following treatment with 17β-estradiol (open columns, Fig. 4a). The rABCG2 mRNA level was reduced by 75.7% by transfection of rABCG2 siRNA-03 into TR-BBB13 cells in the presence of 17β-estradiol (G2-03)[E_2(+), Fig. 4a]. In contrast, the transfection of NC siRNA did not affect the rABCG2 mRNA level in TR-BBB13 cells (NC)[E_2(+), Fig. 4a]. Treatment with siRNA targeted to β-actin decreased the β-actin mRNA level by 57.9 ± 2.2% (mean ± SEM; n = 3) in TR-BBB13 cells, supporting the view that siRNA was successfully transfected into TR-BBB13 cells.

To confirm the selectivity of the inhibitory effects of siRNA, the expression levels of other ABC transporters expressed in BCECs were examined. rABCG2 siRNA-03 did not significantly affect the ABCB1, ABCC1 and ABCG1 mRNA levels in TR-BBB13 cells in either the presence or absence of 17β-estradiol (Figs 4b–d). Following the 17β-estradiol treatment, the ABCB1 mRNA level was increased in TR-BBB13 cells (Fig. 4b), whereas the ABCC1 mRNA level showed a tendency to decrease (Fig. 4c), and the ABCG1 mRNA level was unchanged (Fig. 4d).

Suppression of endogenous rABCG2 protein expression in TR-BBB13 cells by siRNA

The rABCG2 protein expression was suppressed by transfection of rABCG2 siRNA-03 into TR-BBB13 cells (G2-03) compared with untransfected (–) and NC siRNA-transfected (NC) TR-BBB13 cells (Fig. 5a, upper panel). The expression of ABCB1 protein and Na^+,K^+-ATPase protein, used as a standard, was not changed by any of the treatment conditions (Fig. 5a, middle and lower panel, respectively). As shown in Fig. 5(b), the density ratio of rABCG2 to Na^+,K^+-ATPase density was significantly decreased by 62.1% by transfection of rABCG2 siRNA-03 into TR-BBB13 cells (G2-03) compared with untransfected TR-BBB13 cells (–).

Discussion

The present study demonstrated that introduction of any of three rABCG2 siRNAs efficiently decreased the expression of rABCG2 and suppressed the apparent efflux function of mitoxantrone, a substrate drug of rABCG2. Moreover, rABCG2 siRNA selectively suppressed the mRNA and protein expression of rABCG2 in a conditionally immortalized brain capillary endothelial cell line (TR-BBB), an *in vitro* BBB model.

Three of the siRNAs designed to target the rABCG2 gene induced sequence-specific suppression of the expression and function of the rABCG2 transporter (Figs 1–3). None of the siRNAs affected the β-actin protein levels (Fig. 2). This is the first evidence that rABCG2 function can be suppressed by siRNA-induced RNA interference. The differences in efficacy among these three siRNAs could be due to altered ability to silence the rABCG2 gene rather than altered transfection efficiency, because rABCG2 siRNA was present in about 900-fold molar excess over rABCG2-expression plasmid (the amount/length of the rABCG2 siRNA and the plasmid was 3 μg/21 bp and 1 μg/about 6300 bp, respectively). The protein expression and the transport activity of rABCG2 were completely suppressed at 48 h after rABCG2 siRNA-03 transfection (Figs 2 and 3), while reduction of the mRNA expression was around 80% (Fig. 1). This apparent difference may be because the protein level was below the detection threshold of western blot analysis, and below the level required for exerting its function. The expression of

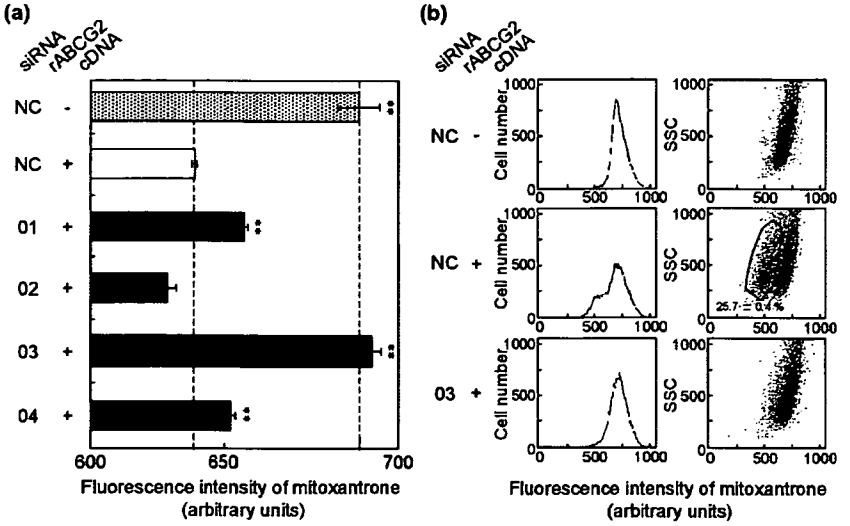

Fig. 3 Effects of rABCG2 siRNAs on mitoxantrone efflux transport in HEK293 cells co-transfected with myc-tagged rABCG2 cDNA. (a) HEK293 cells were transfected with siRNAs (rABCG2 siRNA-01, rABCG2 siRNA-02, rABCG2 siRNA-03 and rABCG2 siRNA-04 (01, 02, 03 and 04) or non-specific control (NC) siRNA) with (+) or without (–) cotransfection of myc-tagged rABCG2 cDNA. The sequences of rABCG2 siRNAs are shown in Table 1. At 48 h after transfection, the cells were incubated with 20 μM mitoxantrone for 1 h at 37°C. Mitoxantrone fluorescence in arbitrary units was determined by flow cytometry with a 635 nm red diode laser and 661 nm bandpass filter. Each column represents the mean ± SEM ($n = 3$). $^{**}p < 0.01$, significantly different from the NC siRNA-treated HEK293 cells co-transfected with myc-tagged rABCG2 cDNA (NC +). (b) Representative histogram plot and dot plot of HEK293 cells transfected with siRNAs [NC siRNA or rABCG2 siRNA-03 (03)] with (+) or without (–) myc-tagged rABCG2 cDNA, showing the mitoxantrone fluorescence vs. cell number and side scattered light (SSC), respectively. The gated cell population (solid line) identified the mitoxantrone-effluxing cells. The number shown is the proportion of total rABCG2-transfected cells contained in the gated cell population (mean ± SEM; $n = 3$).

exogenous rABCG2 protein was also completely suppressed at 24 h and 72 h after rABCG2 siRNA-03 transfection (Fig. 2), indicating that this siRNA remains effective at least from 24 h to 72 h. The sequence of rABCG2 siRNA-03 is 100% identical with the corresponding sequence of mouse ABCG2 (GenBank accession number NM011920). Therefore, this siRNA could be also effective for suppressing the function of mouse ABCG2.

The sequence locations of the effective rABCG2 siRNA-01, rABCG2 siRNA-03 and rABCG2 siRNA-04 (Table 1) were not limited to within 100-nucleotides downstream from the first ATG in contrast to the previous siRNA design (Elbashir *et al.* 2002). This result is in agreement with the recent report indicating that the major determinant of siRNA activity is the target sequence itself, rather than its location (Yoshinari *et al.* 2004). Recently, eight criteria for rational siRNA design for RNA interference were proposed (Reynolds *et al.* 2004). Indeed, the most effective rABCG2 siRNA (rABCG2 siRNA-03) satisfied as many as six of the criteria. For instance, this siRNA has moderate to low G/C content (30–52%), low internal stability of the sense 3′-end (at least three A/U bases at 15–19 nt) and a lack of internal repeats. Moreover, rABCG2 siRNA-03 has 'A' and 'U' at positions 19 and 10, respectively. It has been reported that these sequence-related criteria had a strong impact on improved selection of highly potent siRNAs (the increase in the probability of selecting siRNAs which induce more than 95% gene silencing was 7.2% and 12.8% for A19 and U10, respectively; Reynolds *et al.* 2004).

The present study has demonstrated that the delivery of siRNA suppresses rABCG2 mRNA and protein expression in TR-BBB13 cells (Figs 4a and 5), which are an *in vitro* BBB model expressing functional rABCG2 (Hori *et al.* 2004). There have been reports that the protein and function of targeted transporters were suppressed concomitantly with silencing of the corresponding genes (Wu *et al.* 2003; Nabokina *et al.* 2004; Said *et al.* 2004). Indeed, the endogenous rABCG2 protein level was suppressed in TR-BBB13 cells concomitantly with its gene silencing. rABCG2 siRNA-03 presumably suppresses transport activity of endogenous rABCG2 in TR-BBB13 cells by the reduction of rABCG2 protein level. The rABCG2 siRNA suppressed the induction of the rABCG2 mRNA level by 17β-estradiol to the same level as in untreated cells (Fig. 4a). This result suggests that this siRNA was efficiently delivered into TR-BBB13 cells and blocked the induced gene expression of rABCG2. Further study using labeled siRNA would be useful for distinguishing the transfection efficiency of siRNA from the efficacy of siRNA on endogenous rABCG2.

The rABCG2 mRNA level increased in TR-BBB13 cells following treatment with 100 nM 17β-estradiol (Fig. 4). Estrogen is thought to reach a maximum concentration of

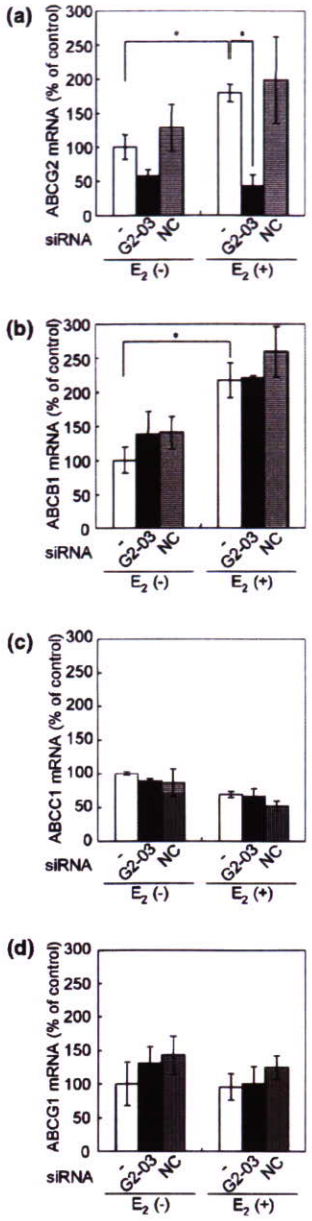

Fig. 4 Selective gene silencing of rABCG2 in TR-BBB13 cells by siRNA.TR-BBB13 cells were transfected with rABCG2 siRNA-03 (G2-03, ■) or non-specific control siRNA (NC, ■), or untransfected (–, □). After 24 h transfection of siRNAs, the culture medium was changed to that with (+) or without (–) 17β-estradiol (E_2), and culture was continued for another 24 h. The ABCG2 (a), ABCB1 (b), ABCC1 (c), and ABCG1 (d) mRNA levels were determined by quantitative real-time PCR analysis. Each column represents the mean ± SEM ($n = 3$). Each mRNA level was normalized relative to the β-actin mRNA level. Each mRNA level is shown as percentage of the mean of the mRNA levels in TR-BBB13 cells treated with non-siRNA (–) and 17β-estradiol (E_2) (the leftmost column). $^*p < 0.05$, significant difference.

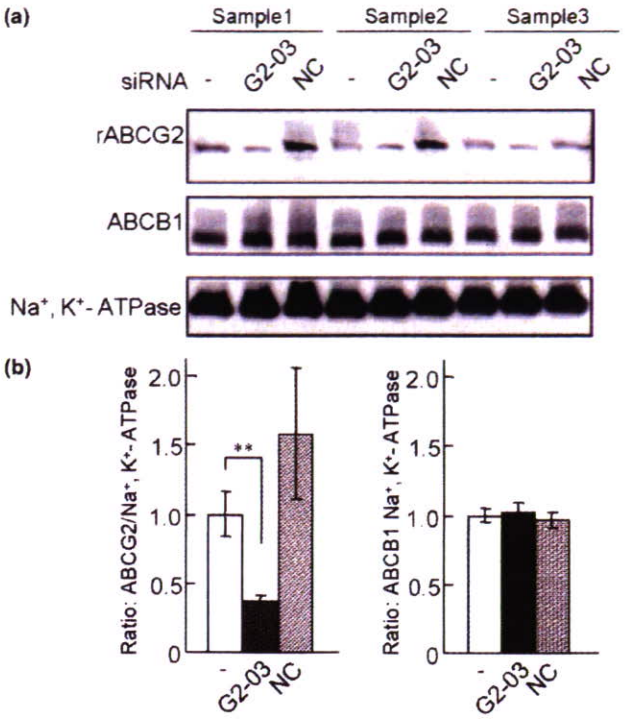

Fig. 5 Selective suppression of rABCG2 protein expression in TR-BBB13 cells by siRNA.TR-BBB13 cells were transfected with rABCG2 siRNA-03 (G2-03) or non-specific control siRNA (NC), or untransfected (–). After 36 h transfection of siRNAs, the cells were collected for western blot analysis using anti-ABCG2, anti-ABCB1 and anti-Na^+,K^+-ATPase antibodies.(a) Results from three independent western blot analyses (samples 1–3) are shown. (b) The ratio of ABCG2 (left panel) or ABCB1 (right panel) densities to Na^+,K^+-ATPase density. Each column represents the mean ± SEM ($n = 3$). $^{**}p < 0.01$, significantly different from untransfected cells (–).

150 nM during the third trimester of pregnancy (Clarke *et al.* 2001). Under such conditions, there is possibility that brain-to-blood transport activity via ABCG2 would be induced. 17β-Estradiol also regulates the expression of ABCB1 and ABCC1 mRNAs in TR-BBB13 cells, suggesting that these ABC transporter-mediated transport systems may be affected by exposure to 17β-estradiol. Recently, it has been reported that the promoter region of human ABCG2 gene contains a novel and functional estrogen response element (ERE) which has 83.3% (10 aa/12 aa) homology with a classical consensus ERE (Ee *et al.* 2004). A search of the rat genome sequence revealed that the first intron of rABCG2 also has a sequence which shows 83.3% (10 aa/12 aa) homology with the classical consensus ERE. It has been reported that 17β-estradiol enhances the ABCG2 mRNA expression in estrogen receptor (ER)-positive human cancer cell lines (Ee *et al.* 2004), and that BCECs express multiple subtypes of ER-α (Stirone *et al.* 2003). Investigation of the sensitivity of the ERE-like sequence should provide a better understanding of the mechanism of rABCG2 induction by 17β-estradiol treatment.

Introduction of siRNA into TR-BBB13 cells would be a promising approach to clarify the specific role of each transporter at the BBB because the cells retain the *in vivo*

transport properties towards various compounds (Terasaki *et al.* 2003). The efficiency of a DNA vector-based transfection using cationic liposomes was less than 5% in TR-BBB13 cells (unpublished data). The present study suggests that oligonucleotide (siRNA)-based transfection is far more effective than DNA vector-based transfection in the case of TR-BBB13 cells. ABCG2 confers multidrug resistance upon cancer cells, so ABCG2 siRNA-induced RNA interference may also be useful for overcoming drug resistance.

The luminal localization of ABCG2 at the BBB has been clearly demonstrated in humans (Cooray *et al.* 2002) and rats (Hori *et al.* 2004). However, the functional contribution of ABCG2 at the BBB *in vivo* remains unclear (Allen and Schinkel 2002). Following rABCG2 siRNA-03 transfection into TR-BBB13 cells, the mRNA level of ABCG1, which has sequence homology with ABCG2, was unchanged (Fig. 4d), and those of ABCB1 and ABCC1, which can transport some ABCG2 substrates, were unaffected for at least 48 h after the siRNA transfection (Figs 4b.c). These data suggest that the silencing effect of the siRNA is specific for the ABCG2 gene in this *in vitro* BBB model. Because the rABCG2 siRNA selectively suppressed rABCG2 mRNA and protein, the siRNA study should allow us to clarify the contribution of the transporter to the BBB efflux transport. Indeed, it has recently been reported that siRNA designed to distinguish thiamine transporter subtypes induced subtype-specific gene silencing in Caco-2 cells, and that the functional contribution of the subtypes to thiamine uptake in the cells was clearly demonstrated by using the siRNA (Said *et al.* 2004). Such a sequence-specific silencing by siRNA may be a promising way to achieve a deeper understanding of the physiological and pharmacological roles of rABCG2 at the BBB. Regarding transporter gene knockdown at the BBB, the siRNA transfection into BCECs should be more specific than suppression by inhibitors, and easier to carry out as compared with the development of knockout mice. Moreover, the siRNA technique would be useful for silencing plural transporter genes because mixtures of siRNAs can be delivered.

In conclusion, the present study has demonstrated that delivery of siRNA into this *in vitro* BBB model specifically reduced endogenous rABCG2 protein level as well as its mRNA level. Application of the siRNA technique to BBB research should increase our understanding of ABCG2 role at the BBB.

Acknowledgements

We wish to thank Prof. M. Watanabe, Mr M. Tachikawa for helpful discussion and establishment of anti-ABCG2 antibody, and Messrs M. Fujiyoshi, N. Kimura for technical assistance. We would also like to thank Ms N. Funayama for secretarial assistance. This study was supported in part by a Grant-in-Aid for Scientific Research from Japan Society for the Promotion of Science, and a 21st Century COE Program Special Research Grant from the Ministry of Education Science, Sports and Culture. It was also supported in part by the Industrial Technology Research Grant Program from the New Energy and Industrial Technology Development Organization (NEDO) of Japan.

References

Allen J. D. and Schinkel A. H. (2002) Multidrug resistance and pharmacological protection mediated by the breast cancer resistance protein (BCRP/ABCG2). *Mol. Cancer Ther.* **1**, 427–434.

Allen J. D., van Loevezijn A., Lakhai J. M., van der Valk M., van Tellingen O., Reid G., Schellens J. H., Koomen G. J. and Schinkel A. H. (2002) Potent and specific inhibition of the breast cancer resistance protein multidrug transporter in vitro and in mouse intestine by a novel analogue of fumitremorgin C. *Mol. Cancer Ther.* **1**, 417–425.

Asaba H., Hosoya K., Takanaga H., Ohtsuki S., Tamura E., Takizawa T. and Terasaki T. (2000) Blood–brain barrier is involved in the efflux transport of a neuroactive steroid, dehydroepiandrosterone sulfate, via organic anion transporting polypeptide 2. *J. Neurochem.* **75**, 1907–1916.

de Bruin M., Miyake K., Litman T., Robey R. and Bates S. E. (1999) Reversal of resistance by GF120918 in cell lines expressing the ABC half-transporter, MXR. *Cancer Lett.* **146**, 117–126.

Clarke R., Leonessa F., Welch J. N. and Skaar T. C. (2001) Cellular and molecular pharmacology of antiestrogen action and resistance. *Pharmacol. Rev.* **53**, 25–71.

Cooray H. C., Blackmore C. G., Maskell L. and Barrand M. A. (2002) Localisation of breast cancer resistance protein in microvessel endothelium of human brain. *Neuroreport* **13**, 2059–2063.

Ee P. L., Kamalakaran S., Tonetti D., He X., Ross D. D. and Beck W. T. (2004) Identification of a novel estrogen response element in the breast cancer resistance protein (ABCG2) gene. *Cancer Res.* **64**, 1247–1251.

Elbashir S. M., Harborth J., Weber K. and Tuschl T. (2002) Analysis of gene function in somatic mammalian cells using small interfering RNAs. *Methods* **26**, 199–213.

Gao B., Stieger B., Noe B., Fritschy J. M. and Meier P. J. (1999) Localization of the organic anion transporting polypeptide 2 (Oatp2) in capillary endothelium and choroid plexus epithelium of rat brain. *J. Histochem. Cytochem.* **47**, 1255–1264.

Hannon G. J. (2002) RNA interference. *Nature* **418**, 244–251.

Hori S., Ohtsuki S., Tachikawa M., Kimura N., Kondo T., Watanabe M., Nakashima E. and Terasaki T. (2004) Functional expression of rat ABCG2 on the luminal side of brain capillaries and its enhancement by astrocyte-derived soluble factor(s). *J. Neurochem.* **90**, 526–536.

Hosoya K., Takashima T., Tetsuka K. *et al.* (2000a) mRNA expression and transport characterization of conditionally immortalized rat brain capillary endothelial cell lines; a new *in vitro* BBB model for drug targeting. *J. Drug Target.* **8**, 357–370.

Hosoya K., Tetsuka K., Nagase K. *et al.* (2000b) Conditionally immortalized brain capillary endothelial cell lines established from a transgenic mouse harboring temperature-sensitive simian virus 40 large T-antigen gene. *AAPS Pharmsci.* **2**, article 27. doi: 10.128/ps020327 Available: http://www.aapspharmsci.org

Hosoya K., Ohtsuki S. and Terasaki T. (2002) Recent advances in the brain-to-blood efflux transport across the blood–brain barrier. *Int. J. Pharm.* **248**, 15–29.

Hyafil F., Vergely C., Du Vignaud P. and Grand-Perret T. (1993) *In vitro* and *in vivo* reversal of multidrug resistance by GF120918, an acridonecarboxamide derivative. *Cancer Res.* **53**, 4595–4602.

Mori S., Takanaga H., Ohtsuki S., Deguchi T., Kang Y. S., Hosoya K. and Terasaki T. (2003) Rat organic anion transporter 3 (rOAT3) is responsible for brain-to-blood efflux of homovanillic acid at the abluminal membrane of brain capillary endothelial cells. *J. Cereb. Blood Flow Metab.* **23**, 432–440.

Nabokina S. M., Ma T. Y. and Said H. M. (2004) Mechanism and regulation of folate uptake by the human pancreatic epithelial MIA PaCa-2 cells. *Am. J. Physiol. Cell Physiol.* **287**, C142–C148.

Rabindran S. K., Ross D. D., Doyle L. A., Yang W. and Greenberger L. M. (2000) Fumitremorgin C reverses multidrug resistance in cells transfected with the breast cancer resistance protein. *Cancer Res.* **60**, 47–50.

Reynolds A., Leake D., Boese Q., Scaringe S., Marshall W. S. and Khvorova A. (2004) Rational siRNA design for RNA interference. *Nat. Biotechnol.* **22**, 326–330.

Said H. M., Balamurugan K., Subramanian V. S. and Marchant J. S. (2004) Expression and functional contribution of hTHTR-2 in thiamine absorption in human intestine. *Am. J. Physiol. Gastrointest. Liver Physiol.* **286**, G491–G498.

Stirone C., Duckles S. P. and Krause D. N. (2003) Multiple forms of estrogen receptor-alpha in cerebral blood vessels: regulation by estrogen. *Am. J. Physiol. Endocrinol. Metab.* **284**, E184–E192.

Suzuki M., Suzuki H., Sugimoto Y. and Sugiyama Y. (2003) ABCG2 transports sulfated conjugates of steroids and xenobiotics. *J. Biol. Chem.* **278**, 22 644–22 649.

Terasaki T. and Hosoya K. (1999) The blood–brain barrier efflux transporters as a detoxifying system for the brain. *Adv. Drug Deliv. Rev.* **36**, 195–209.

Terasaki T., Ohtsuki S., Hori S., Takanaga H., Nakashima E. and Hosoya K. (2003) New approaches to *in vitro* models of blood–brain barrier drug transport. *Drug Discov. Today* **8**, 944–954.

Virgintino D., Robertson D., Errede M., Benagiano V., Girolamo F., Maiorano E., Roncali L. and Bertossi M. (2002) Expression of P-glycoprotein in human cerebral cortex microvessels. *J. Histochem. Cytochem.* **50**, 1671–1676.

Wu H., Hait W. N. and Yang J. M. (2003) Small interfering RNA-induced suppression of MDR1 (P-glycoprotein) restores sensitivity to multidrug-resistant cancer cells. *Cancer Res.* **63**, 1515–1519.

Yoshinari K., Miyagishi M. and Taira K. (2004) Effects on RNAi of the tight structure, sequence and position of the targeted region. *Nucl Acids Res.* **32**, 691–699.

Zelcer N., Reid G., Wielinga P., Kuil A., van der Heijden I., Schuetz J. D. and Borst P. (2003) Steroid and bile acid conjugates are substrates of human multidrug-resistance protein (MRP)4 (ATP-binding cassette C4). *Biochem. J.* **371**, 361–367.

Zhang Y., Boado R. J. and Pardridge W. M. (2003) *In vivo* knockdown of gene expression in brain cancer with intravenous RNAi in adult rats. *J. Gene Med.* **5**, 1039–1045.

doi:10.1111/j.1440-1746.2007.05076.x

HEPATOLOGY

Inhibition of hepatitis C virus infection and expression *in vitro* and *in vivo* by recombinant adenovirus expressing short hairpin RNA

Naoya Sakamoto,*,† Yoko Tanabe,* Takanori Yokota,‡ Kenichi Satoh,§ Yuko Sekine-Osajima,* Mina Nakagawa,*,† Yasuhiro Itsui,* Megumi Tasaka,* Yuki Sakurai,* Chen Cheng-Hsin,* Masahiko Yano,¶ Shogo Ohkoshi,¶ Yutaka Aoyagi,¶ Shinya Maekawa,†† Nobuyuki Enomoto,†† Michinori Kohara§ and Mamoru Watanabe*

Departments of *Gastroenterology and Hepatology, ‡Hepatitis Control, and †Neurology and Neurological Science, Tokyo Medical and Dental University, §Department of Microbiology and Cell Biology, The Tokyo Metropolitan Institute of Medical Science, Tokyo, ¶Gastroenterology and Hepatology Division, Graduate School of Medical and Dental Sciences, Niigata University, Niigata, and ††First Department of Medicine, Yamanashi University, Yamanashi, Japan

Key words
adenovirus vector, hepatitis C virus, RNA interference.

Accepted for publication 12 April 2007.

Correspondence
Dr Naoya Sakamoto, Department of Gastroenterology and Hepatology, Tokyo Medical and Dental University, 1-5-45 Yushima, Bunkyo-ku, Tokyo 113-8519, Japan.
Email: nsakamoto.gast@tmd.ac.jp

NS and YT have contributed equally to this paper.

Abstract

Background and Aim: We have reported previously that synthetic small interfering RNA (siRNA) and DNA-based siRNA expression vectors efficiently and specifically suppress hepatitis C virus (HCV) replication *in vitro*. In this study, we investigated the effects of the siRNA targeting HCV-RNA *in vivo*.

Methods: We constructed recombinant retrovirus and adenovirus expressing short hairpin RNA (shRNA), and transfected into replicon-expressing cells *in vitro* and transgenic mice *in vivo*.

Results: Retroviral transduction of Huh7 cells to express shRNA and subsequent transfection of an HCV replicon into the cells showed that the cells had acquired resistance to HCV replication. Infection of cells expressing the HCV replicon with an adenovirus expressing shRNA resulted in efficient vector delivery and expression of shRNA, leading to suppression of the replicon in the cells by ~10^{-3}. Intravenous delivery of the adenovirus expressing shRNA into transgenic mice that can be induced to express HCV structural proteins by the Cre/*lox*P switching system resulted in specific suppression of virus protein synthesis in the liver.

Conclusion: Taken together, our results support the feasibility of utilizing gene targeting therapy based on siRNA and/or shRNA expression to counteract HCV replication, which might prove valuable in the treatment of hepatitis C.

Introduction

Hepatitis C virus (HCV), which affects 170 million people worldwide, is one of the most important pathogens causing liver-related morbidity and mortality.[1] The difficulty in eradicating HCV is attributable to limited treatment options against the virus and their unsatisfactory efficacies. Even with the most effective regimen with pegylated interferon (IFN) and ribavirin in combination, the efficacies are limited to less than half of the patients treated.[2] Given this situation, the development of safe and effective anti-HCV therapies is one of our high-priority goals.

RNA interference (RNAi) is a process of sequence-specific, post-transcriptional gene silencing that is initiated by double-stranded RNA.[3,4] Because of its potency and specificity, RNAi rapidly has become a powerful tool for basic research to analyze gene functions and for potential therapeutic applications. Recently, successful suppression of various human pathogens by RNAi have been reported, including human immunodeficiency viruses,[5,6] poliovirus,[7] influenza virus,[8] severe acute respiratory syndrome (SARS) virus[9] and hepatitis B virus (HBV).[10–13]

We and other researchers have reported that appropriately designed small interfering RNA (siRNA) targeting HCV genomic RNA can efficiently and specifically suppress HCV replication *in vitro*.[14–19] We have tested siRNA designed to target the well-conserved 5′-untranslated region (5′-UTR) of HCV-RNA, and identified the most effective target, just upstream of the translation initiation codon. Furthermore, transfection of DNA-based vectors expressing siRNA was as effective as that of synthetic siRNA in suppressing HCV replication.[14]

In this study, we explored the further possibility that efficient delivery and expression of siRNA may be effective in suppression and elimination of HCV replication and that delivery of such

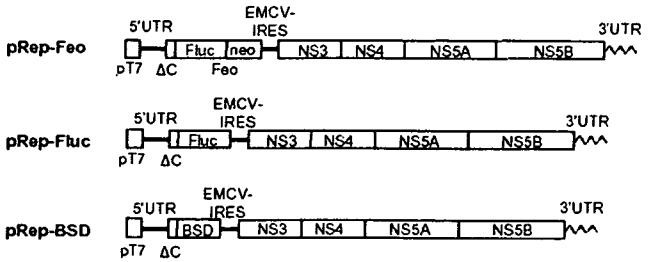

Figure 1 Structures of HCV replicon plasmids. The pRep-Feo expressed a chimeric reporter protein of firefly luciferase (Fluc) and neomycin phosphotransferase (GenBank accession No. AB119282).[14,20] The pRep-Fluc expressed the Fluc protein. The pRep-BSD expressed the blasticidin S (BSD) resistance gene. pT7, T7 promoter; 5'UTR, HCV 5'-untranslated region; ΔC, truncated HCV core region (nt. 342–377); neo, neomycin phosphotransferase gene; EMCV, encephalomyocarditis virus; NS3, NS4, NS5A and NS5B, genes that encode HCV non-structural proteins; 3'UTR, HCV 3'-untranslated region.

HCV-directed siRNA *in vivo* may be effective in silencing viral protein expression in the liver. Here, we report that HCV replication was suppressed *in vitro* by recombinant retrovirus and adenovirus vectors expressing short hairpin RNA (shRNA) and that the delivery of the adenovirus vector to mice *in vivo* specifically inhibited viral protein synthesis in the liver.

Methods

Cells and cell culture

Huh7 and Retro Pack PT67 cells (Clontech, Palo Alto, CA, USA) were maintained in Dulbecco's modified minimal essential medium (Sigma, St. Louis, MO, USA) supplemented with 10% fetal calf serum at 37°C under 5% CO_2. To maintain cell lines carrying the HCV replicon, G418 (Wako, Osaka, Japan) was added to the culture medium to a final concentration of 500 μg/mL.

HCV replicon constructs and transfection

HCV replicon plasmids, pRep-Feo, pRep-Fluc and pRep-BSD were constructed from were constructed from a virus, HCV-N strain, genotype 1b.[21] The pRep-Feo expressed a chimeric reporter protein of firefly luciferase (Fluc) and neomycin phosphotransferase.[14,20] The pRep-Fluc and the pRep-BSD expressed the Fluc and blasticidin S (BSD) resistance genes, respectively (Fig. 1). The replicon RNA synthesis and the transfection protocol have been described previously.[22]

Synthetic siRNA and siRNA-expression plasmid

The design and construction of HCV-directed siRNA vectors have been described.[14] Briefly, five siRNA targeting the 5'-UTR of HCV RNA were tested for their efficiency to inhibit HCV replication, and the most effective sequence, which targeted nucleotide position of 331 though 351, was used in the present study. To construct shRNA-expressing DNA cassettes, oligonucleotide inserts were synthesized that contained the loop sequence (5'-TTC AAG AGA-3') flanked by sense and antisense siRNA sequences (Fig. 2a). These were inserted immediately downstream of the human U6 promoter. To avoid a problem in transcribing shRNA because of instability of the DNA strands arising from the tight palindrome structure, several C-to-T point mutations, which retained completely the silencing activity of the shRNA, were introduced into the sense strand of the shRNA sequences (referred to as 'm').[23] A control plasmid, pUC19-shRNA-Control, expressed shRNA directed towards the Machado–Joseph disease gene, which is a mutant of ataxin-3 gene and is not normally expressed. We have previously described the sequence specific activity of the shRNA-Control.[24]

Prior to construction of the virus vectors, we tested silencing efficiency of five shRNA constructs of different lengths that covered the target sequence (Fig. 2a). The shRNA-HCV-19, shRNA-HCV-21 and shRNA-HCV-27 had target sequences of 19, 21 and 27 nucleotides, respectively. Transfection of these shRNA constructs into Huh7/pRep-Feo showed that shRNA with longer target sequences had better suppressive effects (Fig. 2b). Therefore, we used shRNA-HCV-27m (abbreviated as shRNA-HCV) in the following study.

Recombinant retrovirus vectors

The U6-shRNA expression cassettes were inserted into the *StuI*/*Hin*dIII site of a retrovirus vector, pLNCX2 (Clontech) to construct pLNCshRNA-HCV and pLNCshRNA-Control (Fig. 2c). The plasmids were transfected into the packaging cells, Retro Pack PT67. The culture supernatant was filtered and added onto Huh7 cells with 4 μg/mL of polybrene. Huh7 cell lines stably expressing shRNA were established by culture in the presence of 500 μg/mL of G418.

Recombinant adenovirus

Recombinant adenoviruses expressing shRNA were constructed using an Adenovirus Expression Vector Kit (Takara, Otsu, Japan). The U6-shRNA expression DNA cassette was inserted into the *Swa*I site of pAxcw to construct pAxshRNA-HCV and pAxshRNA-Control. The adenoviruses were propagated according to the manufacturer's protocol (AxshRNA-HCV and AxshRNA-Control; Fig. 2c). A 'multiplicity of infection' (MOI) was used to standardize infecting doses of adenovirus. The MOI stands for the ratio of infectious virus particles to the number of cells being infected. An MOI = 1 represents equivalent dose to introduce one infectious virus particle to every host cell that is present in the culture.

Plasmids for assays of interferon responses

pISRE-TA-Luc (Invitrogen, Carlsbad, CA, USA) contained five copies of the consensus interferon stimulated response element (ISRE) motifs upstream of the Fluc gene. pTA-Luc (Invitrogen), which lacks the enhancer element, was used for background determination. The pcDNA3.1 (Invitrogen) was used as an empty vector for mock transfection. pRL-CMV (Promega, Madison, WI, USA), which expresses the *Renilla* luciferase protein, was used for normalization of transfection efficiency.[25] A plasmid, pcGFPneo (Invitrogen), was used to monitor percentages of transduced cells.

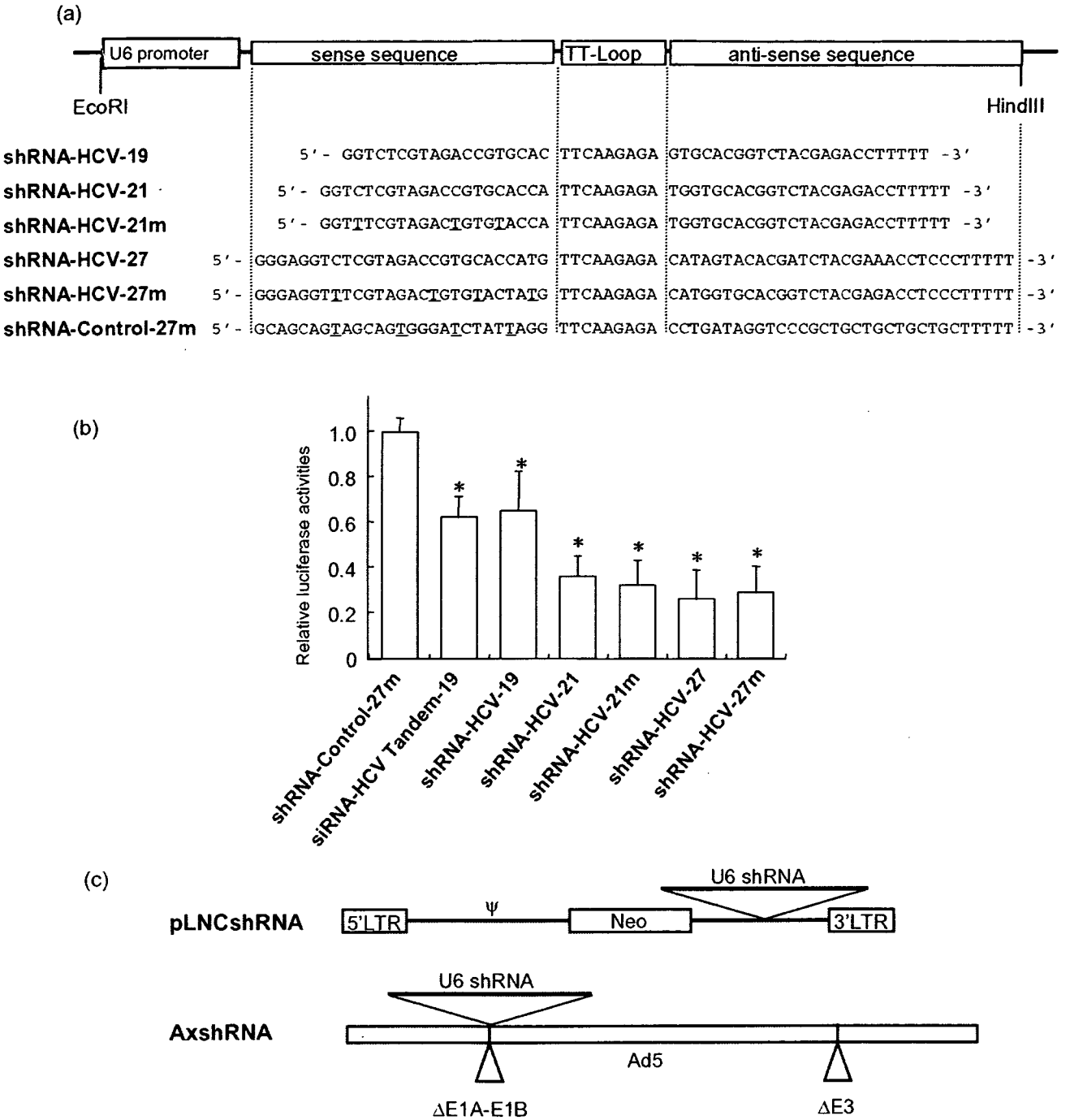

Figure 2 Structure of shRNA-expression constructs and shRNA sequences. (a) Structure of shRNA-expression cassette and shRNA sequences. TT-Loop, the loop sequence. The shRNA-Control was directed toward an unrelated target, Machado–Joseph disease gene. Underlined letters indicate C-to-T point mutations in the sense strand. (b) The shRNA-expression plasmids were transfected into Huh7/pRep-Feo cells, and internal luciferase activities were measured at 48 h of transfection. Each assay was done in triplicate, and the values are displayed as mean + SD. $^*P < 0.05$. (c) pLNCshRNA, structure of a recombinant retrovirus expressing shRNA. Ψ, the retroviral packaging signal sequence. AxshRNA, structure of a recombinant adenovirus expressing shRNA.

Real-time RT-PCR analysis

Total cellular RNA was extracted from cultured cells or liver tissue using ISOGEN (Nippon Gene, Tokyo, Japan). Total cellular RNA (2 μg) was used to generate cDNA from each sample using the SuperScript II reverse-transcriptase (Invitrogen). The mRNA expression levels were measured using the Light Cycler PCR and detection system (Roche, Mannheim, Germany) and Light Cycler Fast Start DNA Master SYBR Green I mix (Roche).

Luciferase assays

Luciferase activity was measured using a luminometer, Lumat LB9501 (Promega) and the Bright-Glo Luciferase Assay System (Promega) or the Dual-Luciferase Reporter Assay System (Promega).

Northern and western hybridization

Total cellular RNA was separated by denaturing agarose-formaldehyde gel electrophoresis, and transferred to a nylon membrane. The membrane was hybridized with a digoxigenin-labeled probe specific for the full-length replicon sequence, and subsequently with a probe specific for beta-actin. The signals were detected by chemiluminescence reaction using a Digoxigenin Luminescent Detection Kit (Roche), and visualized by Fluoro-Imager (Roche). For the western blotting, 10 μg of total cell lysate was separated on NuPAGE 4.12% Bis-TrisGel (Invitrogen), and blotted onto an Immobilon PVDF Membrane (Roche). The membrane was incubated with monoclonal antibodies specific for HCV-NS5A (BioDesign, Saco, ME, USA), NS4A (Virogen, Watertown, MA, USA), or beta-actin (Sigma), and detected by a chemiluminescence reaction (BM Chemiluminescence Blotting Substrate; POD, Roche).

Transient-replication assays

A replicon, pRep-Fluc, was transfected into cells and the luciferase activities of the cell lysates were measured serially. To correct the transfection efficiency, each value was divided by the luciferase activity at 4 h after the transfection.

Stable colony formation assays

Cells were transfected with a replicon, pRep-BSD, and were cultured in the presence of 150 μg/mL of BSD (Invitrogen). BSD-resistant cell colonies appeared after ~3 weeks of culture, and were counted.

HCV-JFH1 virus cell culture

An *in-vitro* transcribed HCV-JFH1 RNA[26] was transfected into Huh7.5.1 cells.[27] Naive Huh7.5.1 cells were subsequently infected by the culture supernatant of the JFH1-RNA transfected Huh-7.5.1 cells, and subjected to siRNA or drug treatments. Replication levels of HCV-RNA were quantified by the realtime RT-PCR by using primers that targeted HCV-NS5B region, HCV-JFH1 sense: 5′-TCA GAC AGA GCC TGA GTC CA-3′, and HCV-JFH1 antisense: 5′-AGT TGC TGG AGG GCT TCT GA-3′.

Mice and adenovirus infection

Transgenic mice, CN2-29, inducibly express mRNA for the HCV structural proteins (genotype1b, nucleotides 294–3435) by the Cre/*lox*P switching system.[28] The transgene does not contain full-length HCV 5′-UTR, but shares the target sequence of the shRNA-HCV. Although the transgenic mouse CN2 has been previously reported as expressing higher levels of the viral proteins, the expression levels of the viral core protein in the CN2-29 mice are modest and similar to that in the liver of HCV patients. Thus, we chose CN2-29 mice in the present study.

The mice were infected with AxshRNA-HCV or controls (AxshRNA-Control or AxCAw1) in combination with AxCAN-Cre, which expressed Cre recombinase. Three days after the infection, the mice were killed and HCV core protein in the liver was measured as described below. The BALB/c mice were maintained in the Animal Care Facility of Tokyo Medial and Dental University, and transgenic mice were in the Tokyo Metropolitan Institute of Medical Science. Animal care was in accordance with institutional guidelines. The review board of the university approved our experimental animal studies and all experiments were approved by the institutional animal study committees.

Measurement of HCV core protein in mouse liver

The amounts of HCV core protein in the liver tissue from the mice was measured by a fluorescence enzyme immunoassay (FEIA)[29] with a slight modification. Briefly, the 5F11 monoclonal anti-HCV-core antibody was used as the first antibody on the solid phase, and the 5E3 antibody conjugated with horseradish peroxidase was the second antibody. This FEIA can detect as little as 4 pg/mL of recombinant HCV-core protein. Contents of the HCV core protein in the liver samples were normalized by the total protein contents and expressed as pg/mg total protein.

Immunohistochemical staining

Liver tissue was frozen with optimal cutting temperature (OTC) compound (Tissue Tek; Sakura Finetechnical, Tokyo, Japan). The sections (8 μm thick) were fixed with a 1:1 solution of acetone : methanol at −20°C for 10 min and then washed with phosphate-buffered saline (PBS). Subsequently, the sections were incubated with the IgG fraction of an anti-HCV core rabbit polyclonal antibody (RR8)[28] in blocking buffer or antialbumin rabbit polyclonal antibody (Dako Cytomation, Glostrup, Denmark) in PBS overnight at 4°C. The sections were incubated with secondary antibody, Alexa-antirabbit IgG (Invitrogen) or TRITIC-antirabbit IgG (Sigma), for 2 h at room temperature. Fluorescence was observed using a fluorescence microscope.

Statistical analyses

Statistical analyses were performed using Student's *t*-test; *P*-values of less than 0.05 were considered to be statistically significant.

Results

Retrovirus transduction of shRNA can protect from HCV replication

Retrovirus vectors propagated from pLNCshRNA-HCV and pLNCshRNA-Control were used to infect Huh7 cells, and cell lines were established that constitutively express shRNA-HCV and shRNA-Control (Huh7/shRNA-HCV and Huh7/shRNA-Control, respectively). There were no differences in the cell morphology or growth rate between shRNA-transduced and non-transduced Huh7 cells (data not shown). The HCV replicon, pRep-Fluc, was transfected into Huh7/shRNA-HCV, Huh7/shRNA-Control and naive Huh7 cells by electroporation. In Huh7/shRNA-Control and naive Huh7 cells, the initial luciferase activity at 4 h decreased temporarily, which represents decay of the transfected replicon RNA, but increased again at 48 h and 72 h, which demonstrate de novo synthesis of the HCV replicon RNA. In contrast, transfection into Huh7/shRNA-HCV cells resulted in a decrease in the initial luciferase activity, reaching background by 72 h (Fig. 3a). Similarly, transfection of the replicon, pRep-BSD, into Huh7 cells and BSD selection yielded numerous BSD-resistant colonies in the naive Huh7 (832 colonies) and Huh7/shRNA-Control cell lines (740 colonies), while transfection of Huh7/shRNA-HCV, which expressed shRNA-HCV, yielded obviously fewer colonies (five colonies), indicating reduction of colony forming units by ~10^2 (Fig. 3b). There was no difference in shape, growth or viability between cells expressing the shRNA or not. These results indicated that cells expressing HCV-directed shRNA following retrovirus transduction acquired resistance to HCV replication.

Effect of recombinant adenoviruses expressing shRNA on *in vitro* HCV replication

We investigated subsequently the effects of recombinant adenovirus vectors expressing shRNA. AxshRNA-HCV and AxshRNA-Control were used separately to infect Huh7/pRep-Feo cells, and the internal luciferase activities were measured sequentially (Fig. 4a). AxshRNA-HCV caused continuous suppression of HCV RNA replication. Six days postinfection, the luciferase activities fell to background levels. In contrast, the luciferase activities of the Huh7/pRep-Feo cells infected with AxshRNA-Control did not show any significant changes compared with untreated Huh7/pRep-Feo cells (Fig. 4a). The dimethylthiazol carboxymethoxyphenyl sulfophenyl tetrazolium (MTS) assay showed no significant difference between cells that were infected by recombinant adenovirus and uninfected cells (Fig. 4b). In the northern blotting analysis, the cells were harvested 6 days after infection with the adenovirus at an MOI of 1. Feo-replicon RNA of 9.6 kb, which was detectable in the untreated Huh7/pRep-Feo cells and in the cells infected with AxshRNA-Control, diminished substantially following infection with the AxshRNA-HCV (Fig. 4c). Densitometries showed that the intracellular levels of the replicon RNA in the Huh7/pRep-Feo cells correlated well with the internal luciferase activities. Similarly in the western blotting, cells were harvested 6 days after infection with adenovirus. Levels of the HCV NS4A and NS5A proteins that were translated from the HCV replicon decreased following infection with the AxshRNA-HCV (Fig. 4d). These results indicated that the decrease in luciferase activities was due to specific suppressive effects of shRNA on expression of HCV genomic RNA and the viral proteins, and not due to non-specific effects caused by the delivery of shRNA or to toxicity of the adenovirus vectors.

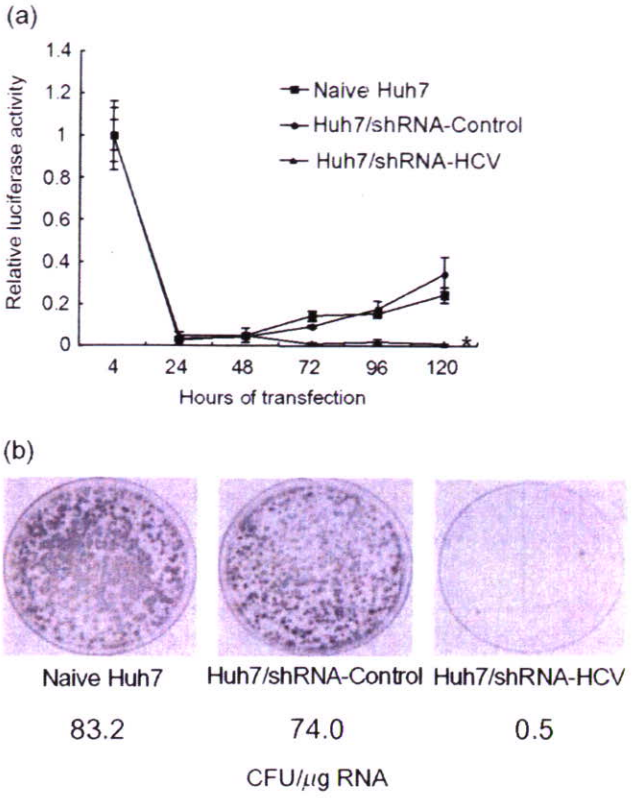

Figure 3 HCV replication can be inhibited by shRNA-HCV which was stably transfected into cells. Huh7/shRNA-HCV and Huh7/shRNA-Control stably express shRNA-HCV or shRNA-Control, respectively, following retroviral transduction. (a) Transient replication assay. An HCV replicon RNA, pRep-Fluc, was transfected into naive Huh7, Huh7/shRNA-HCV and Huh7/shRNA-Control cells. Luciferase activities of the cell lysates were measured serially at the times indicated, and the values were plotted as ratios relative to luciferase activities at 4 h. The luciferase activities at 4 h represent transfected replicon RNA. The data are mean + SD. An asterisk denotes a *P*-value of less than 0.001 compared with the corresponding value of the naive Huh7 cells. (b) Stable colony formation assay. The HCV replicon, pRep-BSD, was transfected into naive Huh7, Huh7/shRNA-HCV and Huh7/shRNA-Control cells. The cells were cultured in the presence of blasticidin S (BSD) in the medium for ~3 weeks, and the BSD-resistant colonies were counted. These assays were repeated twice. The colony-forming units per microgram RNA (CFU/μg RNA) are shown at the bottom.

Absence of interferon-stimulated gene responses by siRNA delivery

It has been reported that double-stranded RNA may induce interferon-stimulated gene (ISG) responses which cause instability of mRNA, translational suppression of proteins and apoptotic cell

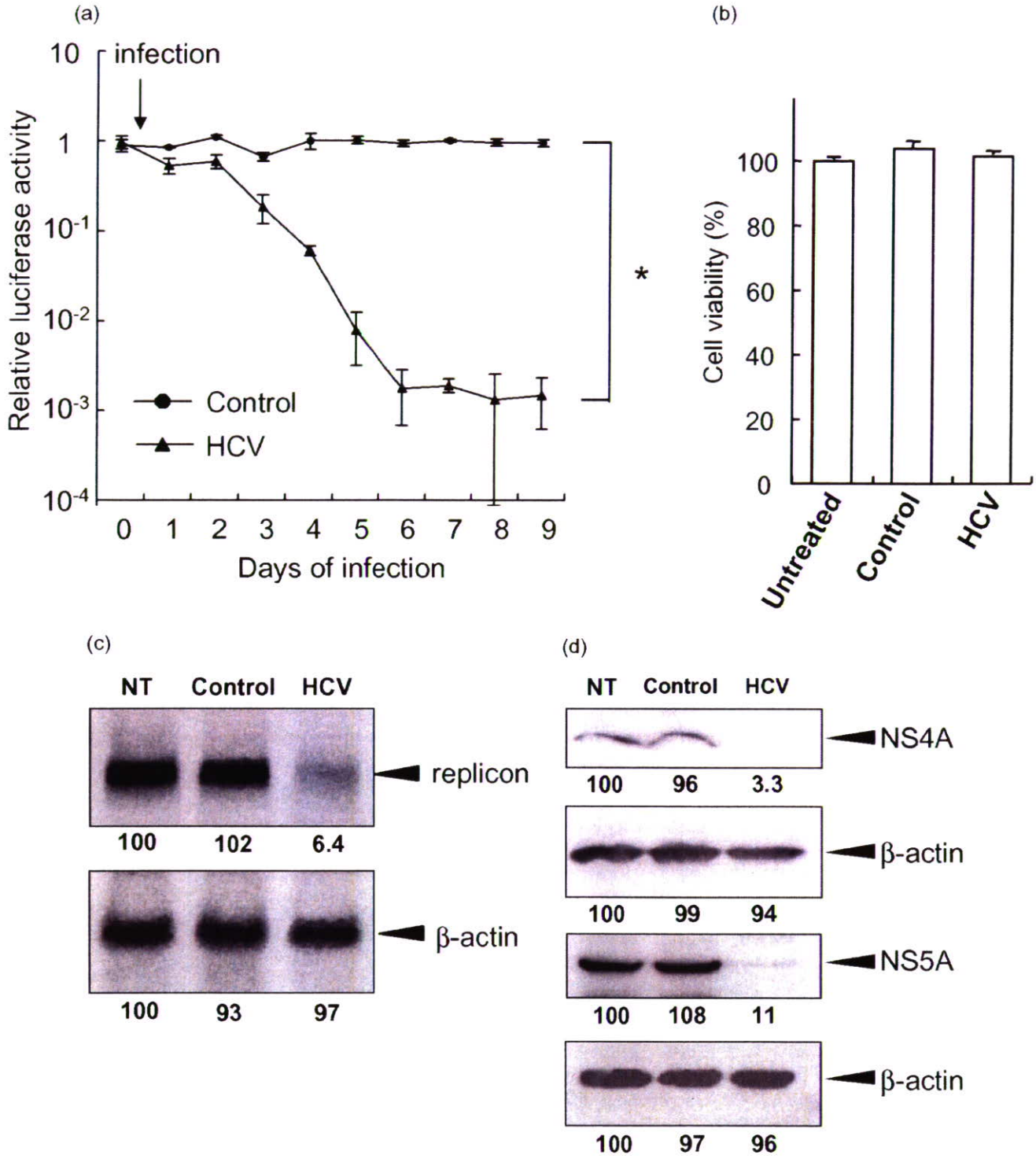

death.[18,30,31] Therefore, we examined the effects of the shRNA-expressing plasmids and adenoviruses on the activation of ISG expression in cells. The ISRE-reporter plasmid, pISRE-TA-Luc, and a control plasmid, peGFPneo, were transfected into Huh7 cells with plasmid pUC19-shRNA-HCV or pUC19-shRNA-Control, or adenovirus, AxshRNA-HCV or AxshRNA-Control, and the ISRE-mediated luciferase activities were measured. On day 2, the ISRE-luciferase activities did not significantly change in cells in which

Figure 4 Effect of a recombinant adenovirus expressing shRNA on HCV replicon. (a) Huh7/pRep-Feo cells were infected with AxshRNA-HCV or shRNA-Control at a multiplicity of infection (MOI) of 1. The cells were harvested, and internal luciferase activities were measured on day 0 though day 9 after adenovirus infection. Each assay was done in triplicate, and the value is displayed as a percentage of no treatment and as mean ± SD. An asterisk indicates a *P*-value of less than 0.05. (b) Dimethylthiazol carboxymethoxyphenyl sulfophenyl tetrazolium (MTS) assay of Huh7/pRep-Feo cells. Cells were infected with indicated recombinant adenoviruses at an MOI of 1. The assay was done at day 6 of infection. Error bars indicate mean + SD. (c) Northern blotting. The upper panel shows replicon RNA, and the lower panel shows beta-actin mRNA. (d) Western blotting. Total cell lysates were separated on NuPAGE gel, blotted and incubated with monoclonal anti-NS4A or anti-NS5A antibodies. The membrane was re-blotted with antibeta-actin antibodies. NT, untreated Huh7/pRep-Feo cells; Control, cells infected with AxshRNA-Control; HCV, cells treated with AxshRNA-HCV. In panels (b) and (c), cells were harvested on day 6 after adenovirus infection at an MOI of 1.

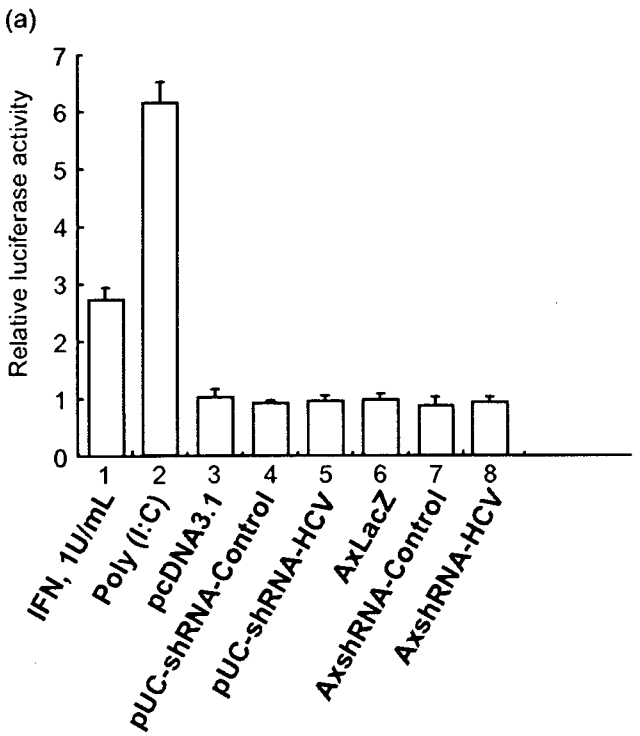

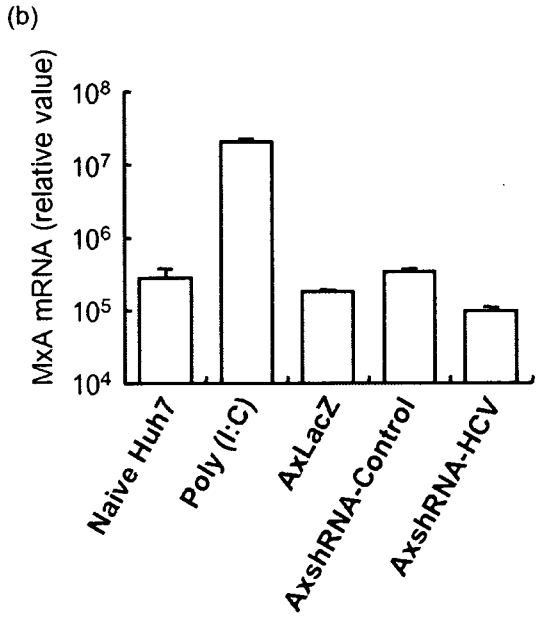

Figure 5 Interferon-stimulated gene responses by transfection of siRNA vectors. (a) Huh7 cells were seeded at 5×10^4 per well in 24-well plates on the day before transfection. As a positive control, 200 ng of pISRE-TA-Luc, or pTA-Luc, 1 ng of pRL-CMV, were transfected into a well using FuGENE-6 Transfection Reagent (Roche), and the cells were cultured with 1 U/mL of interferon (IFN) in the medium (lane 1). Lanes 3–5: 200 ng of pISRE-TA-Luc or pTA-Luc, and 1 ng of pRL-CMV were cotransfected with (lane2) 300 ng of poly (I : C), or 200 ng of plasmids (lane 3) pcDNA3.1, (lane 4) pUC19-shRNA-Control or (lane 5) pUC19-shRNA-HCV. Lanes 6–8: 200 ng of pISRE-TA-Luc or pTA-Luc, and 1 ng of pRL-CMV were transfected, and MOI = 1 of adenoviruses, (lane 6) AxLacZ, which expressed the beta-galactosidase (LacZ) gene under control of the chicken beta-actin (CAG) promoter as a control, (lane 7) AxshRNA-Control or (lane 8) AxshRNA-HCV were infected. Dual luciferase assays were performed at 48 h after transfection. The Fluc activity of each sample was normalized by the respective Rluc activity, and the respective pTA luciferase activity was subtracted from the pISRE luciferase activity. The experiment was done in triplicate, and the data are displayed as means + SD. (b) Huh7 cells were infected with indicated recombinant adenoviruses, AxLacZ, AxshRNA-Control and AxshRNA-HCV. RNA was extracted from each sample at day 6, and mRNA expression levels of an interferon-inducible MxA protein were quantified by the real-time RT-PCR analysis. Primers used were as follows: human MxA sense, 5′-CGA GGG AGA CAG GAC CAT CG-3′; human MxA antisense, 5′-TCT ATC AGG AAG AAC ATT TT-3′; human beta-actin sense, 5′-ACA ATG AAG ATC AAG ATC ATT GCT CCT CCT-3′; and human beta-actin antisense, 5′-TTT GCG GTG GAC GAT GGA GGG GCC GGA CTC-3′.

negative- or positive-control shRNA plasmids was transfected. (Fig. 5a). Similarly, the expression levels of an interferon-inducible MxA protein did not significantly change by transfection of shRNA-expression vectors (Fig. 5b). These results demonstrate that the shRNA used in the present study lack induction of the ISG responses both in the form of the expression plasmids and the adenovirus vectors.

Effect of siRNA and shRNA adenoviruses on HCV-JFH1 cell culture

The effects of HCV-targeted siRNA- and shRNA-expressing adenoviruses were confirmed by using HCV-JFH1 virus cell culture system. Transfection of the siRNA #331[14] into HCV-infected Huh7.5.1 cells resulted in substantial decrease of intracellular HCV RNA, while a control siRNA showed no effect (Fig. 6a). Similarly, infection of AxshRNA-HCV into Huh7.5.1/HCV-JFH1 cells specifically suppressed expression of HCV RNA (Fig. 6b).

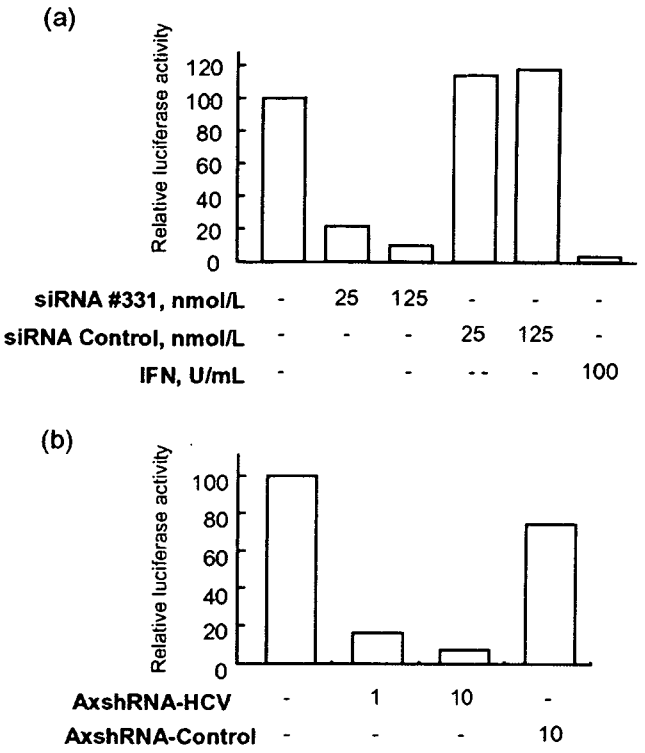

Figure 6 Effects of an siRNA and adenovirus expressing shRNA on HCV-JFH1 cell culture. (a) The siRNA #331, the siRNA-Control[14], (b) AxshRNA-HCV or AxshRNA-Control were, respectively, transfected or infected onto HV-JFH1-infected Huh7.5.1 cells. Seventy-two hours of the transfection or infection, expression level of HCV-RNA was quantified by real-time RT-PCR. The assays were repeated twice, and consistent results were obtained. IFN, recombinant interferon-alpha 2b.

Suppression of HCV-IRES-mediated translation *in vivo* by adenovirus expressing shRNA

The effects of the shRNA expression on the expression of the viral structural proteins *in vivo* were investigated using conditional HCV cDNA-transgenic mice, CN2-29.[28] Adenoviruses, AxshRNA-HCV, AxshRNA-Control or AxCAwl were injected into CN2-29 mice in combination with AxCANCre, an adenovirus expressing *Cre* DNA recombinase. The mice were killed on the fourth day after the injection, and the hepatic expression of the HCV core protein was measured. The expressed amounts of the core protein were 143.0 ± 56.2 pg/mg and 108.5 ± 42.4 pg/mg in AxCAwl and AxshRNA-Control-infected mice, respectively, and the expressed amount was significantly lower in mice injected with AxshRNA-HCV (28.7 ± 7.0 pg/mg, $P < 0.05$, Fig. 7a). Similarly, the induced expression of HCV core protein was not detectable by immunohistochemistry in AxshRNA-HCV infected liver tissue (Fig. 7c). Staining of a host cellular protein, albumin, was not obviously different between the liver infected with AxCAwl, AxshRNA-HCV and AxshRNA-Control (Fig. 7d). The expression levels of two ISG, IFN-beta and Mx1, in the liver tissue were not significantly different between individuals with and without injection of the adenovirus vectors (Fig. 7b). These results indicate specific shRNA silencing of HCV structural protein expression in the liver.

Discussion

The requirements to achieve a high efficiency using RNAi are: (i) selection of target sequences that are the most susceptible to RNAi; (ii) persistence of siRNA activity; and (iii) efficient *in vivo* delivery of siRNA to cells. We have used an shRNA sequence that was derived from a highly efficient siRNA (siRNA331), and constructed a DNA-based shRNA expression cassette that showed competitive effects with the synthetic siRNA (Fig. 2).[14] The shRNA-expression cassette does not only allow extended half-life of the RNAi, but also enables use of gene-delivery vectors, such as virus vectors. As shown in the results, a retrovirus vector expressing shRNA-HCV could stably transduce cells to express HCV-directed shRNA, and the cells acquired protection against HCV subgenomic replication (Fig. 3). An adenovirus vector expressing shRNA-HCV resulted in suppression of HCV subgenomic and protein expression by around three logs to almost background levels (Fig. 4). Consistent results were obtained by using an HCV cell culture (Fig. 6). More importantly, we have demonstrated *in-vivo* effects on viral protein expression in the liver using a conditional transgenic mouse model (Fig. 7). These results suggest that efficient delivery of siRNA could be effective against HCV infection *in vivo*.

An obstacle to applying siRNA technology to treat virus infections is that viruses are prone to mutate during their replication.[32] HCV continuously produces mutated viral strains to escape immune defense mechanisms. Even in a single patient, the circulating HCV population comprises a large number of closely related HCV sequence variants called quasispecies. Therefore, siRNA targeting the protein-coding sequence of the HCV genome, which have been reported by others,[15–19] may vary considerably among different HCV genotypes, and even among strains of the same genotype.[33] Our shRNA sequence targeted the 5′-UTR of HCV RNA, which is the most conserved region among various HCV isolates.[33] In addition, the structural constraints on the 5′-UTR, in terms of its requirement to direct internal ribosome entry and translation of viral proteins, might not permit the evolution of escape mutations. Our preliminary results have shown that the siRNA-HCV suppressed replication of an HCV genotype 2a replicon[34] to the same extent as the HCV 1b replicon.

Although the siRNA techniques rely on a high degree of specificity, several studies report siRNA-induced non-specific effect that may result from induction of ISG responses.[18,31] These effects may be mediated by activation of double-strand RNA-dependent protein kinase, toll-like receptor 3,[35] or possibly by a recently identified RNA helicase, RIG-I.[36] It remains to be determined whether these effects are generally induced by every siRNA construct. Sledz *et al.* have reported that transfection of two siRNA induced cellular interferon responses,[37] while Bridge *et al.* report that shRNA-expressing plasmids induced an interferon response but transfection of synthetic siRNA did not.[31] Speculatively, these effects on the interferon system might be construct dependent. Our shRNA-expression plasmids and adenoviruses did not activate ISG responses *in vitro* (Fig. 5a,b) or *in vivo* (Fig. 7b). We have preliminarily detected phosphorylated PKR (P-PKR) by western

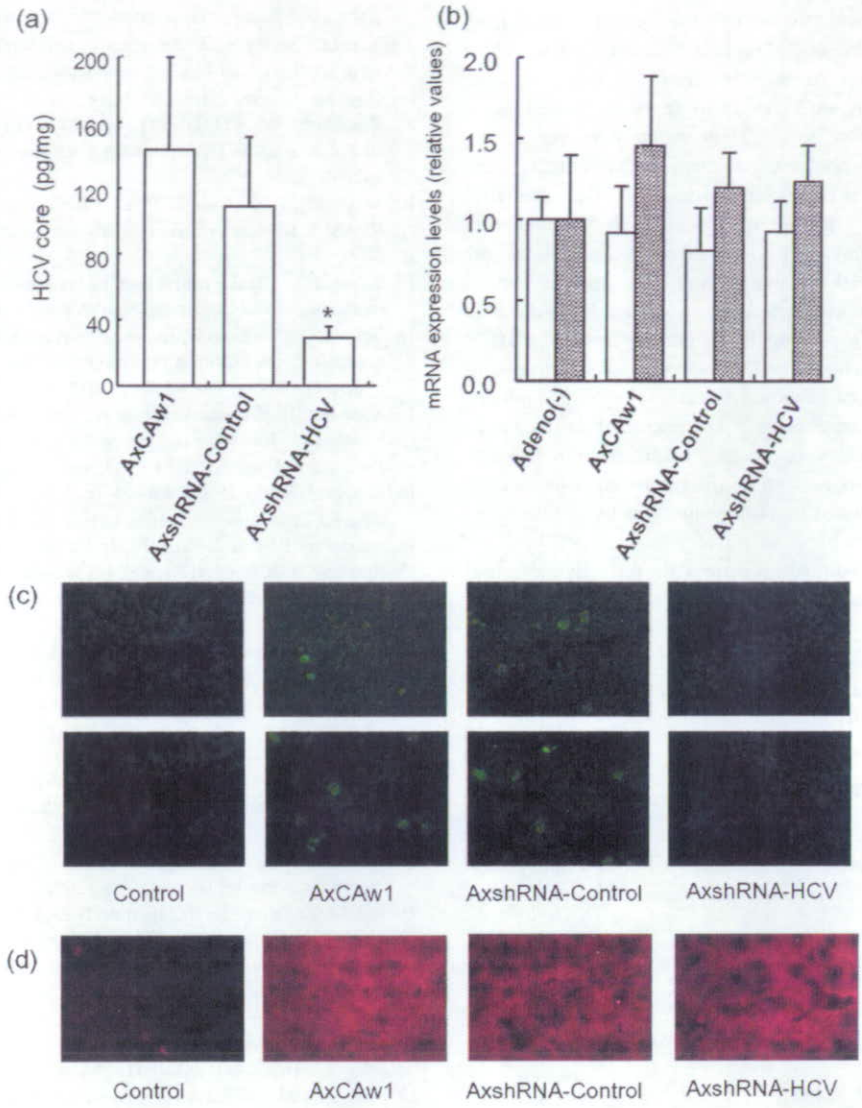

Figure 7 Effects of a recombinant adenovirus expressing shRNA on HCV core protein expression in CN2-29 transgenic mice. CN2-29 transgenic mice were administered with 1×10^9 PFU of AxCANCre combined with 6.7×10^8 PFU of AxshRNA-HCV, AxshRNA or AxCAw1. The mice were killed on day 4 after injection. (a) Quantification of HCV core protein in liver. Liver tissues were homogenized and used to determine the amount of HCV core protein. Each assay was done in triplicate, and the values are displayed as mean ± SD. Asterisk indicates *P*-value of less than 0.05. (b) Expression levels of mouse interferon-beta (white bars) and Mx1 (shaded bars) mRNA in the mouse liver tissue were quantified by the real-time RT-PCR analyses. Primers used were as follows: mouse interferon-beta sense, 5′-ACA GCC CTC TCC ATC AAC TA-3′; mouse interferon-beta antisense, 5′-CCC TCC AGT AAT AGC TCT TC-3′; mouse Mx1 sense, 5′-AGG AGT GGA GAG GCA AAG TC-3′; mouse Mx1 antisense, 5′-CAC ATT GCT GGG GAC TAC CA-3′; mouse beta-actin sense, 5′-ACT CCT ATG TGG GTG ACG AG-3′; mouse beta-actin antisense, 5′-ATA GCC CTC GTA GAT GGG CA-3′. Adeno (-) denotes mice without adenovirus administration. (c) Immunofluorescence microscopy of HCV core protein in the liver tissue. Liver sections of mice were stained using rabbit anticore polyclonal antibody and normal rabbit IgG as a negative control. The upper photographs were obtained at 400× magnification, and the lower photographs were at 1000×. (d) Immunofluorescence microscopy of albumin in liver. Liver sections from the mice were fixed and stained using rabbit antialbumin antibody and normal rabbit IgG as a negative control.

blotting, and found no apparent increase of P-PKR (data not shown). These results indicate that these target sequences and structures are of sufficient specificity to silence the target gene without eliciting non-specific interferon responses.

Beside the canonical action of siRNA, a sequence-specific cleavage of target mRNA, the siRNA could act as a micro-RNA that suppresses translational initiation of mRNA,[38] or it could mediate transcriptional gene silencing.[39] Regarding our *in-vivo* experiments, it was difficult to differentially analyze the effect of siRNA at individual sites of action because post-translational effect of siRNA concomitantly destabilizes target mRNA, which leads to apparent decrease of mRNA transcripts.

Efficiency and safety of gene transfer methods are the key determinants of the clinical success of gene therapy and an unresolved problem. There are several reports of delivery of siRNA or siRNA-expression vectors to cells *in vivo*;[12,40,41] however, gene delivery methods that are safe enough to apply to clinical therapeutics are currently under development. Adenovirus vectors are one of the most commonly used carriers for human gene therapies.[42–44] Our present results demonstrate that the adenoviral delivery of shRNA is effective in blocking HCV replication *in vitro* and virus protein expression *in vivo*. Adenovirus vectors have several advantages of efficient delivery of transgene both *in vitro* and *in vivo* and natural hepatotropism when administered *in vivo*. The AxshRNA-HCV specifically blocked expression of HCV structural proteins in a conditional transgenic mouse expressing those proteins. The current adenovirus vectors may cause inflammatory reactions in the target organ,[45] however, and produce neutralizing antibodies which make repeated administration difficult. These problems may be overcome by the improved constructs of virus vectors with attenuated immunogenicity or by the development of non-viral carriers for gene delivery.[46]

In conclusion, our results demonstrate the effectiveness and feasibility of the siRNA expression system. The efficiency of adenovirus expressing shRNA that target HCV suggests that delivery and expression of siRNA in hepatocytes may eliminate the virus and that this RNA-targeting approach might provide a potentially effective future therapeutic option for HCV infection.

Acknowledgments

This study was supported by grants from Japan Society for the Promotion of Science, 15590629 and 16590580, and partly supported by a grant from the Viral Hepatitis Research Foundation of Japan.

References

1 Alter MJ. Epidemiology of hepatitis C. *Hepatology* 1997; **26**: 62S–65S.
2 Hadziyannis SJ, Sette H Jr, Morgan TR *et al.* Peginterferon-alpha2a and ribavirin combination therapy in chronic hepatitis C: a randomized study of treatment duration and ribavirin dose. *Ann. Intern. Med.* 2004; **140**: 346–55.
3 Fire A, Xu S, Montgomery M, Kostas S, Driver S, Mello C. Potent and specific genetic interference by double-stranded RNA in Caenorhabditis elegans. *Nature* 1998; **19**: 806–11.
4 Elbashir SM, Harborth J, Lendeckel W, Yalcin A, Weber K, Tuschl T. Duplexes of 21-nucleotide RNAs mediate RNA interference in cultured mammalian cells. *Nature* 2001; **411**: 494–8.
5 Coburn GA, Cullen BR. Potent and specific inhibition of human immunodeficiency virus type 1 replication by RNA interference. *J. Virol.* 2002; **76**: 9225–31.
6 Jacque JM, Triques K, Stevenson M. Modulation of HIV-1 replication by RNA interference. *Nature* 2002; **418**: 435–8.
7 Gitlin L, Karelsky S, Andino R. Short interfering RNA confers intracellular antiviral immunity in human cells. *Nature* 2002; **418**: 430–4.
8 Ge Q, Filip L, Bai A, Nguyen T, Eisen HN, Chen J. Inhibition of influenza virus production in virus-infected mice by RNA interference. *Proc. Natl. Acad. Sci. USA* 2004; **101**: 8676–81.
9 Wang C, Pflugheber J, Sumpter R Jr *et al.* Alpha interferon induces distinct translational control programs to suppress hepatitis C virus RNA replication. *J. Virol.* 2003; **77**: 3898–912.
10 Klein C, Bock CT, Wedemeyer H *et al.* Inhibition of hepatitis B virus replication in vivo by nucleoside analogues and siRNA. *Gastroenterology* 2003; **125**: 9–18.
11 Konishi M, Wu CH, Wu GY. Inhibition of HBV replication by siRNA in a stable HBV-producing cell line. *Hepatology* 2003; **38**: 842–50.
12 McCaffrey AP, Meuse L, Pham TT, Conklin DS, Hannon GJ, Kay MA. RNA interference in adult mice. *Nature* 2002; **418**: 38–9.
13 Shlomai A, Shaul Y. Inhibition of hepatitis B virus expression and replication by RNA interference. *Hepatology* 2003; **37**: 764–70.
14 Yokota T, Sakamoto N, Enomoto N *et al.* Inhibition of intracellular hepatitis C virus replication by synthetic and vector-derived small interfering RNAs. *EMBO Rep.* 2003; **4**: 602–8.
15 Kapadia SB, Brideau-Andersen A, Chisari FV. Interference of hepatitis C virus RNA replication by short interfering RNAs. *Proc. Natl. Acad. Sci. USA* 2003; **100**: 2014–18.
16 Kronke J, Kittler R, Buchholz F *et al.* Alternative approaches for efficient inhibition of hepatitis C virus RNA replication by small interfering RNAs. *J. Virol.* 2004; **78**: 3436–46.
17 Randall G, Grakoui A, Rice CM. Clearance of replicating hepatitis C virus replicon RNAs in cell culture by small interfering RNAs. *Proc. Natl. Acad. Sci. USA* 2003; **100**: 235–40.
18 Seo MY, Abrignani S, Houghton M, Han JH. Letter to the editor: small interfering RNA-mediated inhibition of hepatitis C virus replication in the human hepatoma cell line Huh-7. *J. Virol.* 2003; **77**: 810–12.
19 Wilson JA, Jayasena S, Khvorova A *et al.* RNA interference blocks gene expression and RNA synthesis from hepatitis C replicons propagated in human liver cells. *Proc. Natl. Acad. Sci. USA* 2003; **100**: 2783–8.
20 Guo JT, Bichko VV, Seeger C. Effect of alpha interferon on the hepatitis C virus replicon. *J. Virol.* 2001; **75**: 8516–23.
21 Tanabe Y, Sakamoto N, Enomoto N *et al.* Synergistic inhibition of intracellular hepatitis C virus replication by combination of ribavirin and interferon-alpha. *J. Infect. Dis.* 2004; **189**: 1129–39.
22 Maekawa S, Enomoto N, Sakamoto N *et al.* Introduction of NS5A mutations enables subgenomic HCV-replicon derived from chimpanzee-infectious HC-J4 isolate to replicate efficiently in Huh-7 cells. *J. Viral. Hepat.* 2004; **11**: 394–403.
23 Miyagishi M, Sumimoto H, Miyoshi H, Kawakami Y, Taira K. Optimization of an siRNA-expression system with an improved hairpin and its significant suppressive effects in mammalian cells. *J. Gene Med.* 2004; **6**: 715–23.
24 Li Y, Yokota T, Matsumura R, Taira K, Mizusawa H. Sequence-dependent and independent inhibition specific for mutant ataxin-3 by small interfering RNA. *Ann. Neurol.* 2004; **56**: 124–9.
25 Kanazawa N, Kurosaki M, Sakamoto N *et al.* Regulation of hepatitis C virus replication by interferon regulatory factor-1. *J. Virol.* 2004; **78**: 9713–20.
26 Wakita T, Pietschmann T, Kato T *et al.* Production of infectious hepatitis C virus in tissue culture from a cloned viral genome. *Nat. Med.* 2005; **11**: 791–6.
27 Zhong J, Gastaminza P, Cheng G *et al.* Robust hepatitis C virus infection in vitro. *Proc. Natl. Acad. Sci. USA* 2005; **102**: 9294–9.
28 Wakita T, Taya C, Katsume A *et al.* Efficient conditional transgene expression in hepatitis C virus cDNA transgenic mice mediated by the Cre/loxP system. *J. Biol. Chem.* 1998; **273**: 9001–6.
29 Kashiwakuma T, Hasegawa A, Kajita T *et al.* Detection of hepatitis C virus specific core protein in serum of patients by a sensitive fluorescence enzyme immunoassay (FEIA). *J. Immunol. Methods* 1996; **28**: 79–89.

30 Baglioni C, Nilsen TW. Mechanisms of antiviral action of interferon. *Interferon* 1983; **5**: 23–42.
31 Bridge A, Pebernard S, Ducraux A, Nicoulaz A, Iggo R. Induction of an interferon response by RNAi vectors in mammalian cells. *Nat. Genet.* 2003; **34**: 263–4.
32 Carmichael GG. Silencing viruses with RNA. *Nature* 2002; **418**: 379–80.
33 Okamoto H, Okada S, Sugiyama Y *et al.* Nucleotide sequence of the genomic RNA of hepatitis C virus isolated from a human carrier: comparison with reported isolates for conserved and divergent regions. *J. Gen. Virol.* 1991; **72**: 2697–704.
34 Kato T, Date T, Miyamoto M *et al.* Efficient replication of the genotype 2a hepatitis C virus subgenomic replicon. *Gastroenterology* 2003; **125**: 1808–17.
35 Alexopoulou L, Holt AC, Medzhitov R, Flavell RA. Recognition of double-stranded RNA and activation of NF-kB by Toll-like receptor 3. *Nature* 2001; **413**: 732–8.
36 Yoneyama M, Kikuchi M, Natsukawa T *et al.* The RNA helicase RIG-I has an essential function in double-stranded RNA-induced innate antiviral responses. *Nat. Immunol.* 2004; **5**: 730–7.
37 Sledz C, Holko M, de Veer M, Silverman R, Williams, B. Activation of the interferon system by short-interfering RNAs. *Nat. Cell. Biol.* 2003; **5**: 834–9.
38 Doench JG, Petersen CP, Sharp PA. siRNAs can function as miRNAs. *Genes Dev.* 2003; **17**: 438–42.
39 Morris KV. siRNA-mediated transcriptional gene silencing: the potential mechanism and a possible role in the histone code. *Cell. Mol. Life Sci.* 2005; **62**: 3057–66.
40 Xia H, Mao Q, Paulson HL, Davidson BL. siRNA-mediated gene silencing in vitro and in vivo. *Nat. Biotechnol.* 2002; **20**: 1006–10.
41 Zender L, Hutker S, Liedtke C *et al.* Caspase 8 small interfering RNA prevents acute liver failure in mice. *Proc. Natl. Acad. Sci. USA* 2003; **100**: 7797–802.
42 Akli S, Caillaud C, Vigne E *et al.* Transfer of a foreign gene into the brain using adenovirus vectors. *Nat. Genet.* 1993; **3**: 224–8.
43 Bajocchi G, Feldman SH, Crystal RG, Mastrangeli A. Direct in vivo gene transfer to ependymal cells in the central nervous system using recombinant adenovirus vectors. *Nat. Genet.* 1993; **3**: 229–34.
44 Davidson BL, Allen ED, Kozarsky KF, Wilson JM, Roessler BJ. A model system for in vivo gene transfer into the central nervous system using an adenoviral vector. *Nat. Genet.* 1993; **3**: 219–23.
45 Yang Y, Wilson JM. Clearance of adenovirus-infected hepatocytes by MHC class I-restricted CD4+ CTLs in vivo. *J. Immunol.* 1995; **155**: 2564–70.
46 Fleury S, Driscoll R, Simeoni E *et al.* Helper-dependent adenovirus vectors devoid of all viral genes cause less myocardial inflammation compared with first-generation adenovirus vectors. *Basic Res. Cardiol.* 2004; **99**: 247–56.

〔ウイルス　第55巻　第1号，pp.1-8，2005〕

総　説

1. RNAiを用いたウイルス複製抑制

横田　隆徳
東京医科歯科大学院　脳神経機能病態

RNA interference（RNAi）は2本鎖RNAiによって誘導される配列特異的な遺伝子発現抑制である．その中間産物であるShort interfering RNA（siRNA）は哺乳動物細胞においても，インターフェロン反応などの副反応なく目的の遺伝子を切断でき，治験段階に入っているアンチセンス核酸やライボザイムより，有効性，配列特異性いずれもはるかに優れている．その核酸医薬として臨床応用は特にウイルス性疾患において進行している．OFF-Target効果やデリバリー方法などまだまだ解決すべき問題点も多いが，siRNAの高い可能性から種々の方面において医療分野への応用が急速に進展していくことは間違いないものと思われる．

1. RNAiとは

今日までのウイルス増殖抑制の方法はワクチンかウイルス蛋白やウイルス特異酵素をターゲットとした創薬であった．ここ数年，ウイルスゲノム複製に関わる転写，翻訳を核酸レベルで直接抑制しようという試みが，アンチセンス核酸，ライボザイム，DNAエンザイムなどで行われていたが，十分な抑制効果は得られなかった．最近，新しい遺伝子発現抑制（gene silencing）として，これらをはるかに凌ぐ効果を持つRNA interference（RNAi）が注目されている．

長い2本鎖RNAiによって誘導される遺伝子発現抑制であるRNAi現象は植物から昆虫，哺乳動物にいたるまで広く保存して観察され，元来，真核細胞に備わった抗ウイルス機構として知られていた．細胞内に導入された2本鎖RNAはDicerと呼ばれるRNase III核酸分解酵素ファミリーによって21-24merの短い3'突出型の2本鎖RNAであるshort interference RNA（siRNA）に分解される．siRNAはアンチセンス鎖のみがとくほぐされて，ヘリケースなどの蛋白質から成るRNA蛋白質複合体であるRISC複合体（RNA-induced silencing complex）に取り込まれ，アンチセンス鎖に相補的な配列を持つターゲットRNAをその中央で分解する．しかし，哺乳動物における2本鎖RNAの導入はPKRや2' 5' oligosynthetaseの活性化による非特異的な翻訳抑制やRNAの分解が生じ，ホストの細胞の死んでしまうため，分子生物学的手法としても遺伝子治療の方法としてもRNAiの利用の大きな妨げになっていた．しかし，2000年に，RNAi機構の中間産物であるsiRNAを合成して用いることによってこれらの副反応が回避され，siRNAの配列に特異的な遺伝子発現抑制が可能となった[1]．さらに，siRNA配列を短い9merのループ配列でつないだstem型のパリンドロミックなsiRNA配列をpol III系のプロモーター下に挿入したsiRNA発現DNAプラスミドも開発された[2]．また，近年，加えてsiRNAの新たな遺伝子発現抑制機構としてsiRNAを介したDNAの主にプロモーター領域のCpGアイランドをターゲットにメチル化が転写抑制を起こすことも明らかになっている[3]．

RNAi機構は酵母からヒトに至るまで多くの生物種で保存されていて，その生物学的な意義としてはウィルスなどに対する防御機構として進化してきたという仮説が提唱されている．siRNAの発見以来，すぐにいくつかのウイルスにおいて，細胞内でのウイルス遺伝子の切断やウイルス遺伝子複製モデルにおいてsiRNAが有効であるとの報告が相次いでいる．現在まで，エイズウイルス(HIV)[4]，C型[5-8]・B型[9,10]肝炎ウイルス，ポリオウイルス[11]，インフルエンザウイルス[12,13]，ウエストナイルウイルス[13] SARSウイルス，ウエストナイルウイルスを含むの多くウイルスで

連絡先
〒113-8519　東京都文京区湯島1-5-45
TEL：03-5803-5234
FAX：03-5803-0169
E-mail：tak-yokota.nuro@tmd.ac.jp